

Article

Flowback cleanup mechanisms of post-hydraulic fracturing in unconventional natural gas reservoirs

Nasriani, Hamid Reza and Jamiolahmady, Mahmoud

Available at <http://clock.uclan.ac.uk/28293/>

Nasriani, Hamid Reza ORCID: 0000-0001-9556-7218 and Jamiolahmady, Mahmoud (2019) Flowback cleanup mechanisms of post-hydraulic fracturing in unconventional natural gas reservoirs. Journal of Natural Gas Science and Engineering, 66 . pp. 316-342. ISSN 1875-5100

It is advisable to refer to the publisher's version if you intend to cite from the work.
<http://dx.doi.org/10.1016/j.jngse.2019.04.006>

For more information about UCLan's research in this area go to <http://www.uclan.ac.uk/researchgroups/> and search for <name of research Group>.

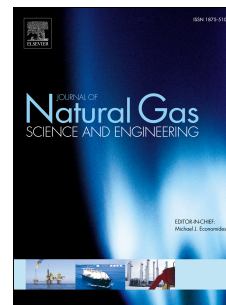
For information about Research generally at UCLan please go to <http://www.uclan.ac.uk/research/>

All outputs in CLoK are protected by Intellectual Property Rights law, including Copyright law. Copyright, IPR and Moral Rights for the works on this site are retained by the individual authors and/or other copyright owners. Terms and conditions for use of this material are defined in the <http://clock.uclan.ac.uk/policies/>

Accepted Manuscript

Flowback cleanup mechanisms of post-hydraulic fracturing in unconventional natural gas reservoirs

Hamid Reza Nasriani, Mahmoud Jamiolahmady



PII: S1875-5100(19)30101-5

DOI: <https://doi.org/10.1016/j.jngse.2019.04.006>

Reference: JNGSE 2870

To appear in: *Journal of Natural Gas Science and Engineering*

Received Date: 25 September 2018

Revised Date: 11 March 2019

Accepted Date: 7 April 2019

Please cite this article as: Nasriani, H.R., Jamiolahmady, M., Flowback cleanup mechanisms of post-hydraulic fracturing in unconventional natural gas reservoirs, *Journal of Natural Gas Science & Engineering*, <https://doi.org/10.1016/j.jngse.2019.04.006>.

This is a PDF file of an unedited manuscript that has been accepted for publication. As a service to our customers we are providing this early version of the manuscript. The manuscript will undergo copyediting, typesetting, and review of the resulting proof before it is published in its final form. Please note that during the production process errors may be discovered which could affect the content, and all legal disclaimers that apply to the journal pertain.

Flowback cleanup mechanisms of post-hydraulic fracturing in unconventional natural gas reservoirs

Hamid Reza Nasriani*¹, Mahmoud Jamiolahmady²

¹University of Central Lancashire, Faculty of Science and Technology, School of Engineering, Preston, United Kingdom

²Heriot-Watt University, Institute of Petroleum Engineering, Edinburgh, United Kingdom

Abstract

This work investigates the fracturing fluid cleanup mechanisms of post-hydraulic fracturing in unconventional gas formations by studying a large number of wide-ranging parameters simultaneously.

In this work, different scenarios of the cleanup operation of the hydraulic fracturing process are considered. This study consists of investigating the post-fracturing cleanup operation of hydraulically fractured vertical wells (VW) and multiple fractured horizontal wells (MFHWs). Additionally, the impact of soaking time, the range of the matrix permeability, applied drawdown pressure, injected fracturing fluid (FF) volume, fracture spacing and horizontal well length has been investigated by running different sets.

Results show that the trend of the impact of relevant parameters for VWs and MFHWs are analogous excepting the matrix permeability, k_m . That is, in the MFHW base reference set, the effect of matrix permeability on capillary pressure is more significant than that on fluid flow while the reverse is observed for VW. The difference in the impact of k_m in VWs and MFHWs is attributed to the geometry of the fluid flow towards the production well and different well completion scheme.

It is also concluded that the impact of parameters affecting the capillary pressure in the matrix is more significant for MFHWs whereas matrix and fracture mobility pertinent parameters are more important for VWs than MFHWs. As a result, larger matrix capillary pressure values are more vital in the cleanup of MFHWs because of more imbibition of FF into the matrix and subsequently lower conflict between the flow of gas and FF in the fracture.

The other part of this research concentrates on the impact of IFT reducing agents on the post-fracturing production in different formations. In hydraulic fracturing operations, these agents

33 are commonly used as an additive in fracturing fluid to facilitate its backflow by reducing Pc
34 and subsequently enhancing gas production. The results of this work recommend that using
35 such agents enhances the gas production rate for ultratight formations but not for tight
36 formations (it reduces the gas production rate). Therefore it is not suggested to use such
37 agents in tight formations.

38 The findings of this work improve the understanding of fracture cleanup leading to better
39 design of hydraulic fracturing operations in unconventional formations.

40

41 **Keywords:** Hydraulic Fracturing; Fracking; Cleanup; unconventional fields; Flowback;
42 fracturing fluid; Multiple Fractured Horizontal Well, Hydraulically Fractured Vertical Well

43

44

45 **1. Introduction & Literature Review**

46 Natural gas is considered to be the cleanest fossil fuel with the least emissions. It is also
47 considered to be one of the most substantial sources of energy in the future due to its
48 abundance and environmental reliability. Natural gas plays a progressively important role in
49 residential heating, industrial, commercial and electrical generation sectors across the world.
50 Natural gas resources could be either conventional or unconventional. Unlike the
51 conventional natural gas reserves that are considered to be one of the most economical and
52 most accessible reserves to extract, unconventional natural gas resources are much more
53 problematic and less economically viable to develop. Coalbed methane, tight and ultra-tight
54 gas sands, gas shales and gas hydrates are considered as unconventional gas resources.
55 Significant demand growth on natural gas has resulted in the development of natural gas
56 resources from tight and ultra-tight gas sands, and shale gas plays. Tight and ultra-tight gas
57 resources make up 57-59% of the unconventional global resources with pronounced
58 abundance in several parts of the world, i.e., Europe, Asia, North Africa, North America and
59 the Middle East, (Dong et al., 2011).

60 Hydraulic fracturing is generally implemented for the productivity enhancement of the wells
61 in the unconventional formations (Clark, 1949; Garrison, 1945; Height, 1944; Lee, 1939).
62 The initiation and propagation of fractures in unconventional reservoirs are achieved through
63 the injection of high volumes of fracturing fluid, FF (Holditch, 1979; Montgomery *et al.*,
64 1990;). Initially, vertically drilled, hydraulically fractured wells in the tight oil and gas fields
65 have been drilled in the North-eastern state of Pennsylvania in the United States. Several field

66 experiences have shown that ineffective FF cleanup can significantly impair gas production.
67 There are several experimental, numerical and field studies investigating the impact of the
68 cleanup efficiency of hydraulic fractures on gas production and FF flowback in
69 unconventional tight/ultra-tight formations (e.g. Pope *et al.*, 1996; Gdanski *et al.*, 2005).
70 The volume of the flowback depends on the characteristic of the formation, FF physical
71 property and the design of the hydraulic fracturing operation. The volume of the flowback
72 that is recovered from the well at the surface could vary from 10% to 70% of the total volume
73 of the FF that was initially injected. Usually, the existence of natural minor fractures in the
74 formation and also having higher matrix capillary pressures could result in retaining more FF
75 in the formation and consequently less flowback recovery at the surface.
76 Nowadays, the optimisation of the fracturing fluid flowback is becoming increasingly
77 important in the oil and gas industry for various reasons. *Tech-Flo Consulting* (2019) utilises
78 a Tech-Flo hydraulic jet pump for FF flowback removal to optimise the load recovery. This
79 technology could accelerate the safe recovery of a large volume of flowback with
80 simultaneous separation of the hydrocarbon from the well stream. *Halliburton* (2018) has
81 also introduced CALIBR engineered flowback service in MFHWs of unconventional fields to
82 improve the well performance by mitigating the completion damage and optimising the
83 longstanding production. CALIBR is an iterative procedure that optimises the well results by
84 continually measuring, analysing and regulating the flowback in order to improve completion
85 efficiency and enhance the well productivity. Using CALIBR could avoid destructive
86 flowback approaches and mitigate the loss in fracture conductivity and impaired well
87 performance by continuously measuring the bottom-hole pressure, analysing the well
88 performance and real-time management of the choke.
89 Holditch (1979) conducted a study on the impact of damage to matrix grids in the
90 surrounding area of the fracture, by examining the effect of FF (considered as water)
91 saturation increase and permeability decrease in near fracture region, on the fractured wells'
92 productivity. He conducted his study employing a finite difference numerical simulator. It
93 was noted that the impact of capillary pressure, P_c , in tight formations (low permeability
94 reservoirs) was evident in low-pressure drawdown (DP) cases in which DP was not
95 significantly larger than the matrix P_c . He described that water blockage happens once the
96 matrix permeability of fracture surrounding region decreases by 99.9% or DP does not
97 become more than P_c in the region invaded by FF. He reported that the FF invasion depth in
98 their matrix was up to 5 in, with uniform FF distribution in the matrix adjacent to the

99 hydraulic fracture. He concluded that in low permeability formations, P_c and relative
100 permeability in invaded zones are significantly important on cleanup efficiency but in his
101 work, the impact of FF volume on the conductivity of the fracture was not investigated.
102 Pope et al. (1996) presented a positive relationship between load recovery and gas production
103 from field data. They explained that as FF is produced back to the surface from HF, an
104 equivalent space in the fracture becomes available to the flow of the gas toward the well.
105 Therefore, the higher the load recovery, the more the gas production. They presented a
106 correlation between FF flowback and gas production rates to support their theory. They also
107 highlighted more substantial initial flow rates would result in load FF recovery.
108 Gdanski *et al.*, (2005) extended the study conducted by Holditch (1979) on cleanup to
109 further investigate the gas and FF two-phase flow and matrix permeability damage in the
110 invaded region. For this study, they developed a numerical model and discussed that the
111 damage in the fracture sand-face extensively reduced gas productivity if k_m in the invaded
112 region is reduced to 1% of the initial permeability of the matrix. They also reported that the
113 larger the original matrix P_c , the more damage to the gas production. However, they did not
114 consider the fact that in the case of larger P_c , FF is imbibed more in the matrix, reducing the
115 FF saturation in the fracture grids, increased gas effective permeability inside the fracture and
116 consequently cleaner fractures.
117 Ghahri et al. (2009) studied the impact of various parameters affecting cleanup efficiency of
118 single fractured vertical wells, VW, of gas and gas-condensate fields. They also reproduced
119 the numerical model results mentioned by Holditch (1979) which has been referred to in
120 many cleanup simulation studies from then on. They reported that the existence of FF in the
121 invaded region affects the cumulative gas production by impairing the gas relative
122 permeability, i.e., it results in a gas production loss compared to a case when no FF was
123 injected. Decreasing the FF viscosity and consequently increasing FF mobility results in more
124 substantial FF recovery at the production stage.
125 They also highlighted that when P_c increases, the FF invades deeper into matrix resulting in
126 improved gas production less impeded by FF
127 Ghahri et al. (2011) extended this work by conducting a wide-ranging analysis of 16 practical
128 parameters simultaneously employing experimental design together with the methodology of
129 response surface (RSM). They demonstrated that gas production loss, GPL, is significantly
130 affected by factors associated with the FF cleanup within the fracture mainly k_f .

131 It should be highlighted that these two numerical studies, i.e., (Ghahri et al., 2011, 2009), the
132 required central processing unit (CPU) time was too long. Consequently, the authors were
133 able to study only two simulations' sets. To facilitate the studying of more different cleanup
134 scenarios, Jamiolahmady et al., (2014) further investigated the flowback cleanup
135 mechanisms, they decreased the number of parameters from 16 to just 12 parameters by
136 removing four parameters that had the slightest impacts on the cleanup performance. These
137 parameters were: the permeability in the matrix and the fracture, interfacial tension, pore size
138 index, and the exponents and endpoints of the Brooks Corey relative permeability correlation
139 for matrix and the fracture (Brooks and Corey, 1964). This work, which was also part of the
140 Heriot-Watt University Gas condensate recovery research was then extended to more
141 different cases of cleanup scenarios in tight and ultra-tight gas formations by conducting 84
142 different sets of simulations. Different factors that had a significant impact on the cleanup
143 efficiency, i.e., injected FF volumes, soaking time, bottom-hole flowing pressure, tightness of
144 the formation, were considered. It was noticed that if the formation becomes tighter (smaller
145 k_m), it results in a more substantial loss in the gas production and consequently, the cleanup
146 procedure will become slower and vice versa. It was also concluded that if the pressure
147 drawdown is small, the impact of P_c on the clean-up performance was more significant, a
148 similar observation was noted once the soaking time was extended (Nasriani, 2017; Nasriani
149 et al., 2018, 2014b, 2014a, Nasriani and Jamiolahmady, 2018a, 2018b).

150 Nasriani et al. (2018) captured the impact of injected fracture fluid volume, length of the
151 fracture, pressure drawdown, hysteresis, layering, gravity segregation and
152 mobility/immobility of the formation water on the post-fracturing cleanup performance. They
153 reported that if a large volume of FF is injected into ultra-tight formations, it results in a
154 substantial gas production loss and hinders the cleanup process intensely. In such a case, the
155 impact of changing other parameters like soaking time extension or pressure drawdown
156 increase improved GPL insignificantly. They showed that hysteresis has an insignificant
157 impact on the cleanup efficiency. They also studied the impact of layered systems on the
158 cleanup performance; they identified that the fluid mobility coefficient within the fracture is
159 meaningfully more significant in the top layer than those of the bottom layer while capillary
160 pressure becomes more significant in bottom layer in comparison with the top layers. They
161 also reported that in cases with high water saturation in the reservoir, the injection of IFT
162 reducing agent could alleviate the gas production loss corresponding to fracturing operation.

163

164 **1.1. The purpose of this study**

165 Most of the previous studies considered the cleanup efficacy of hydraulically fractured
166 vertical wells (VWs). The present study covers a broader area of investigations of the post-
167 fracturing cleanup operation in multiple fractured horizontal wells (MFHWs). More
168 specifically, the impact of considering different fracture spacing and different horizontal
169 lengths in MFHWs on the cleanup efficiency is discussed. It also presents a comparison
170 between the post-fracturing cleanup operation in VWs and MFHWs. It should be noted that it
171 took very long CPU time to conduct the numerical simulation for MFHW sets. Therefore a
172 new sampling approach (Latin Hypercube Sampling (LHS) method) is introduced to reduce
173 the long CPU time required for simulation runs based on full factorial sampling (FFS)
174 experimental design that was implemented in some of the studies mentioned in the previous
175 section.

176 It should be noted that some of the conclusions are due to assumptions or limitations in the
177 model. Permeability and porosity were considered constant and uniform throughout the
178 model to limit the number of variables and reduce the complexity of the model. Additionally,
179 independent variations of the twelve parameters were considered without using dependency
180 function between them.

181

182 **2. Methodology**

183 It is a challenging task to conduct and then analyse a large number of different simulation
184 runs using statistical experimental designs methods and consequently a methodical approach
185 is needed.

186 In this section, the adopted analysis methods and terminologies are explained using a
187 flowchart. Figure 1 represents a Flowchart that explains the workflow of the study of the
188 mechanisms of the cleanup after the fracturing stage. As it is shown, a vertical well (VW)
189 model that was developed initially by Ghahri et al. (2009) was used for VW sets, the
190 validation process of the modified VW model is described elsewhere (Nasriani and
191 Jamiolahmady, 2018a).

192 In addition to the VW model, a new numerical model is developed for MFHW. As it is
193 shown in Figure 1, once the two VW and MFHW models were validated, four scenarios are
194 considered. It is worth mentioning that in each scenario, one or several simulation sets were
195 conducted. The four different scenarios are:

- 196 Scenario 1. VW Base reference set
197 Scenario 2. MFHW Base reference set
198 Scenario 3. MFHW sets with different shutin times, k_m , drawdown pressures and
199 injected fracture fluid
200 Scenario 4. MFHW sets with different fracture spacing and horizontal length

201 In the first two scenarios (i.e., VW base reference set and MFHW base reference set), the
202 full factorial sampling (FFS) was adopted to conduct the required number of numerical
203 simulations. Next, an accurate model, based on the mathematical surface methodology, was
204 matched to the outputs of each set, and consequently, the outcomes of these sets were studied.

205 The FSS data sampling approach that was used to study the cleanup efficiency takes a long
206 CPU (Central Processing Unit) time to conduct numerous runs (i.e. 4096 runs for each set).
207 Introducing more complexity to the models, i.e., changing the numerical model from VW to
208 MFHW, made the CPU time significantly longer. With the intention of decreasing the
209 required number of runs and consequently reducing the CPU time, Latin Hypercube
210 Sampling (LHS) method was used and verified. Consequently, LHS was applied to the
211 MFHW scenarios to create the input to the simulation models. It is worth noting that several
212 simulation sets were conducted in Scenario 3 and 4 for the MFHW case with Latin
213 Hypercube Sampling (LHS) method.

214
215

216 **2.1. Construction, Modification and Validation of MFHW and VW Models**

217 In order to investigate the cleanup operation of vertical (VW) and multiple fractured
218 horizontal wells (MFHW), six different models were set up using ECLIPSE 100
219 (Schlumberger, 2015). The six different models were: a pre-fractured single vertical well
220 model and a new model with three, seven, nine and 13 fractures placed on the 600 m
221 horizontal well length to capture the effect of fracture spacing on the cleanup performance.
222 Additionally, a new MFHW model with ten fractures placed on the 900 m horizontal well
223 length was set up to capture the impact of horizontal length on cleanup efficiency. The local
224 grid refinement (LGR), rather than global refinement was used around fractures in the
225 construction of MFHWs. The application of LGR enabled the authors to capture the impact
226 of the variation of flow parameters in the stimulated reservoir volume while not increasing
227 the CPU time significantly.

228 The initial pressure of the model and the average matrix porosity are 7500 psi and 15%,
229 correspondingly. The numerical models' dimensions are listed in Table 1. Figure 2 presents
230 the section of VW model that is modelled. The set numbers refer to the order they were run
231 as part of a much bigger set of simulations, not all of which are discussed here.

232 The fracking fluid (FF) is considered water. The corresponding viscosity and
233 compressibility for FF were considered 0.5 cp and 0.000005 (1/psia) respectively. For the
234 duration of the hydraulic fracturing phase, the injected FF volume was considered as of twice
235 the volume of the fracture in the sets that is assumed as the base reference sets for VW and
236 MFHW cases. In the next stage of the numerical modelling (post-fracturing stage), gas and
237 FF were produced under a controlled bottom-hole flowing pressure. It should be noted that
238 just after the FF injection stage and before flowback production, a two-day well shut-in
239 period was allowed.

240 It was mentioned previously that the validation process and the governing equations for
241 the modified VW model are described elsewhere (Nasriani and Jamiolahmady, 2018a). The
242 same validation technique was used for the MFHW model. Therefore, to authenticate the
243 developed model for MFHW for the post-fracturing cleanup research, the well bottom-hole
244 pressures versus production time that was predicted by numerical simulation of the MFHW
245 model were compared with the same results from an analytical model for MFHW as that of
246 previously used for VW model by Nasriani and Jamiolahmady (2018b).

247 Figure 3 displays the well bottom-hole pressure (P_{wf}) that is predicted by the simulation
248 model and that forecasted by the analytical model versus production time. It is noted that the
249 two curves are overlapping and laying on top of each other, which confirms the integrity of
250 the simulation model.

251 It should be noted that twelve relevant parameters affecting the post-fracturing cleanup
252 mechanisms are considered in this study. The first eight parameters out of the 12 are the
253 exponents and endpoints of Brooks-Corey (for two different phases) relative permeability
254 correlation.

255 Three parameters control capillary pressure in the matrix, i.e., matrix permeability (k_m),
256 interfacial tension (IFT) and distribution index of the pore size (λ). The last parameter is
257 fracture permeability, k_f .

258 The ranges of the variation of these parameters are presented in Table 2. It should be
259 highlighted that there are six parameters listed in Table 2 that are considered constant

260 throughout a simulation set, i.e., drawdown pressure, matrix porosity, the gas and water
261 critical saturations in both fracture and matrix.

262 Equations 1 & 2 represent the threshold (entry) pressure and capillary pressure (Brooks
263 and Corey, 1966; Thomas et al., 1968). The relative permeability correlation for water and
264 gas are described by Equations 3 & 4 (Brooks and Corey, 1966). It should be noted that in each
265 run of any simulation set, the data are taken within the ranges of the variation of the pertinent
266 parameters that are listed in Table 2 based on a sampling technique, i.e., FFS or LHS.

$$\frac{Pd}{IFT} = 0.0075 \times K^{-0.5}$$

- Threshold pressure Pd, bar 1
- Surface tension IFT (dyne/cm)
- The permeability of the matrix (K (mD))

$$\left(\frac{Pd}{Pc}\right)^\lambda = \frac{S_w - S_{wr}}{1 - S_{wr}} \quad 2$$

$$k_{rw} = K_{\max w} \times \left(\frac{S_w - S_{wr}}{1 - S_{wr} - S_{gr}}\right)^{nw} \quad 3$$

$$k_{rg} = K_{\max g} \times \left(\frac{S_g - S_{gr}}{1 - S_{wr} - S_{gr}}\right)^{ng} \quad 4$$

267
268 To capture the impact of pressure drop (DP) on the cleanup mechanisms, different sets of
269 simulation sets are considered for each DP as noted in Table 3.a and b. It should be
270 highlighted that in this study, the 12 pertinent parameters are scaled between zero and one,
271 zero corresponds to the minimum, and one corresponds to the upper bound, this makes the
272 analysis of the cleanup mechanisms more efficient by response surface methodology (RSM).

273

274 2.2. Response Surface Methodology (RSM) and the main output

275 In this study, Gas Production Loss (GPL, %), which is used as the output, is expressed as
276 the ratio of the difference between the cumulative fracture productions of the situation with
277 an undamaged (totally clean from FF) fracture and damaged (unclean) fracture cumulative
278 production to the undamaged (totally clean) fracture cumulative productions.

$$GPL = 100 \times \left[\frac{FGPT_{\text{clean}} - FGPT_{\text{unclean}}}{FGPT_{\text{clean}}} \right] \quad 5$$

FGPT: total gas cumulative production

279

280 It is very difficult, or technically impossible, to have an entirely clean (undamaged)
 281 fracture after hydraulic fracturing operation. However, if the related parameters and their
 282 impact on post-fracturing operations are well understood then real field strategies regarding
 283 the fracturing operations could be further improved to attain a much cleaner fracture with
 284 enhanced productivity. It should be noted that this main response, i.e. GPL is a normalised
 285 parameter; making it easier to compare different scenarios. In the current study, the effect of
 286 the 12 parameters as mentioned earlier on gas production loss is captured using the tornado
 287 charts. In this approach, if a parameter has a positive influence on the cleanup efficiency, it
 288 reduces the gas production loss (GPL) or in other words more cumulative gas production
 289 when the value of the parameter is raised. Conversely, if a parameter has a negative influence
 290 on the cleanup efficiency, it increases the gas production loss (GPL) or in other words less
 291 cumulative gas production when the value of the parameter is raised.

292 In order to analyse that how sensitive some pertinent parameters are to a particular main
 293 output (main response), response surface methodology is widely used. In statistics and
 294 mathematics, response surface methodology finds an authentic relationship among several
 295 independent parameters, i.e., $x_1, x_2, x_3 \dots x_n$ and the main response variable (y or $f(x_i)$).

296 The RSM, i.e., the fitted polynomial function $f(x_i)$, RSM is defined by Equation 6.

$$y = a_0 + \sum_{k=1}^n a_k x_k + \sum_{i=1}^n \sum_{j=i+1}^n a_i a_j x_i x_j + \sum_{l=1}^n a_l x_l^2 \quad 6$$

297 Equation 6 presents four different models of RSM:

- 298 • Linear Response Surface model (LRSM) that considers (a_0) and $(a_k x_k)$.
- 299 • Linear Response Surface Model with Interaction (ILRSM), if $(a_i a_j x_i x_j)$ are
 300 considered in addition to constant (a_0) and linear terms $(a_k x_k)$ terms.
- 301 • Pure Quadratic Response Surface model (PQRSM) that considers (a_0) and $(a_k x_k)$
 302 and quadratic terms $(a_l^2 x_l^2)$.
- 303 • Full Quadratic Response Surface model (FQRSM) which considers (a_0) , $(a_k x_k)$ and
 304 $(a_l^2 x_l^2)$.

305 In this study, Interactive Linear Response Surface (ILRSM) and Full Quadratic Response
 306 Surface (FQRSM) models were used to obtain GPL as a function of those 12 relevant
 307 parameters for two-level full factorial sampling (FFS), and Latin hypercube sampling (LHS)
 308 approaches respectively. Two different codes, i.e., a MATLAB code (The MathWorks, 2013)
 309 and a Python code, were developed to run all simulations of a simulation set including the pre
 310 and post-processing phases of the fracturing operation.

311

312 **2.3. Analysis Methodology**

313 This work analyses a total of 31 different sets for fractured vertical wells (2 sets) and
314 Multiple fractured horizontal wells (29 sets). It should be noted that all sets use similar
315 reservoir dimensions, however, differ in pressure drawdown, horizontal length, number of
316 fractures (fracture spacing), matrix permeability, shut-in time and the volume of injected FF.
317 A full list of those different sets is shown in Table 3a and 3b. As it is shown in Table 3a and
318 3b, there are two base reference sets for VW and MFHW respectively. The two base
319 reference sets consider the 12 relevant parameters with default ranges as shown in these two
320 tables. New sets are named according to the dissimilarities of the variation range of
321 parameters compared to the base reference set. In Table 3a & b, if a parameter is tick marked,
322 the default variation range is considered for that particular parameter; otherwise, a new
323 variation range is introduced.

324

325 **3. Results and Analyses**

326 **3.1. The Vertical Well Base Case Scenario**

327 Nasriani and Jamiolahmady (2018b) have comprehensively explained the vertical well
328 base reference set, so in this study, a summary of the key findings are reported. For this set,
329 the impact of pertinent parameters on GPL after 10, 30 and 375 days of production is
330 displayed graphically in the form of a tornado chart, Figure 4.

331 Figure 4 shows that the permeability of the fracture, i.e., k_f , has a crucial role in fracture
332 cleanup operation, it has the largest absolute coefficient value of one in the corresponding
333 chart, i.e., the higher k_f results in cleaner fracture and less gas production loss. It should be
334 noted that a large absolute coefficient for the endpoint and exponent (n_{wf} and k_{maxwf}) of
335 Brooks and Corey's correlation (1966) is observed which is in line with having a large
336 absolute value for the k_f coefficient. These observations, i.e., having large absolute
337 coefficient values for k_f , n_{wf} and k_{maxwf} , highlight that the efficiency of the post-fracturing
338 cleanup could be improved if the FF mobility within the fracture is increased. From the data
339 of Figure 4, it is also noted that an increase in the Corey exponents corresponding to gas in
340 both matrix and fracture, i.e., n_{gf} & n_{gm} , impairs the post-fracturing cleanup performance.
341 That means an increase in the mobility of gas within both matrix and fracture results in a
342 decrease in GPL and vice versa.

343 From the data of Figure 4, it is indicated that a decrease in IFT or an increase in λ
344 increases GPL. If Equations 1 and two are considered, a reduction in IFT or a rise in λ reduce
345 the capillary pressure (P_c). Accordingly, it could be concluded that if P_c is increased, cleanup
346 efficiency could improve, as higher P_c allows more FF to be imbibed further into the matrix
347 which this leaves the fracture cleaner for gas to move through it. Notwithstanding the P_c also
348 depends on k_m in addition to IFT and λ , which is discussed next.

349 Figure 4 shows that k_m has a negative coefficient; this suggests that larger k_m results in
350 smaller GPL values. However, it should be noted that k_m has two diverse effects on GPL as
351 follow:

352 (i) An increase in k_m provides better fluid mobility throughout the injection and
353 production stages.

354 (ii) An increase in k_m decreases P_c , which leads to a rise in GPL.

355 It is worth mentioning that the impact of k_m on the improvement of the mobility of the
356 fluid is more dominant than that of the decreasing P_c for this set. Therefore, an increase in k_m
357 resulted in a better cleanup performance. These findings recommend that in the base
358 reference set, the application of chemicals to decrease IFT and consequently to decrease P_c
359 could rise GPL and harm cleanup efficacy and productivity.

360

361 **3.2. Multiple Fractured Horizontal Well set**

362 In this section, the clean-up efficiency of the MFHW set is discussed, and its results are
363 compared with those of the corresponding VW set.

364 As mentioned before, for the case of MFHW, a new model was set-up with three fractures
365 placed on the 600 m horizontal well length. Fracture half-length was 90 m rather than 400 m
366 corresponding to the VW reference set.

367 It is interesting to note that the direction of the impact of parameters is similar except for
368 k_m if the tornado charts of the VW-Set and MFHW set 1 (Figure 4) are considered. That is; in
369 the MFHW set the effect of k_m on P_c is more dominant than that on fluid flow while the
370 reverse is observed for the VW set. VW and MFHW are different in two ways. First the
371 number and volume of fractures and second the position of a fracture concerning the well,
372 resulting in different flow geometries.

373 In order to identify which of these two resulted in this trend change, a new vertical well
374 model (with well competed in the Y-direction, referred to hereafter as Y-VW) was set-up.
375 This Y-VW has a similar well trajectory as that of MFHW. That is, this model is similar to

376 the original VW set up completed in the z-direction (referred to, in this section, as Z-VW)
377 but with the well completed in the Y-direction (rather than Z-direction used for the original
378 VW set, (Figure 5).

379 Figure 9 represents the cumulative frequency of GPL runs of the VW and MFHW base
380 reference set in a histogram chart. In the histogram chart for VW set, if GPL value of 20% is
381 considered, it is noted that after ten days of production, 83% of the numerical simulations
382 have GPL values higher than 20% and 17% less than 20% GPL. At longer production times,
383 i.e., 30 and 365 days, the GPL values decline noticeably, that means that the frequency of
384 runs that have GPL values more than twenty per cent is around 68% and 28% respectively.
385 Therefore it is concluded that as production time increases it results in a better cleanup.

386

387 Comparing tornado charts of the VW-Set 1 (Figure 4) and Y-VW set (Figure 6), it is noted
388 that the k_m trend in the Y-VW case is different from that of the Z-VW Set. This observation
389 indicates that the trend change of k_m is due to the change in the flow geometry and how the
390 well is completed. It should be noted that in the Y-VW set, the area perpendicular to flow at
391 the wellbore is $2\pi r_w * w_f$, which is much less than that, i.e. $H * w_f$, for the Z-VW set, Figure 5.
392 In other words, the connection area between fracture and well is significantly restricted in the
393 Y-VW case. Hence, for the Y-VW set, the effect of flow from the matrix towards fracture
394 during the backflow clean-up is less critical and rather imbibition of fracture fluid governed
395 by matrix capillary pressure, which depends on k_m , is more important.

396 Economides and Martin (2010), reported a similar observation when they investigated the
397 productivity index of different completions, i.e., horizontal transverse, horizontal longitudinal
398 and vertically fractured completions. They referred to a near wellbore choking effect, which
399 is caused by the minimal area of contact between fractures and wellbore and it can seriously
400 affect the productivity of gas wells.

401 To further investigate this observation, Figure 7 and Figure 8 were prepared that show GPL
402 and the gas to FF flow rate ratio vs numbers of runs for Z- and Y-VW cases. These results
403 further confirm that due to a smaller flow area for the Y-VW set, there is more GPL while
404 there is more gas production for the Z-VW set at the same FF production rate. In other words,
405 at the same FF flowback volumes, FF has a more detrimental impact on gas production in the
406 Y-VW case than the Z-VW case due to very restricted connection area between the well and
407 the fracture in Y-VW case.

408 Based on these, it can be concluded that the k_m trend change between VW and MFHWS
409 sets is due to fracture-wellbore flow area connection between these two sets.

410 Figure 9 highlights how fast is the cleanup in MFHW-Sets 1 compared to VW-Set 1 using
411 a histogram chart. Faster clean-up is observed for the MFHW set compared to the VW set.
412 This observation is due to the higher production rate of the MFHW resulting in a faster and
413 more efficient clean-up.

414 In Figure 9, it is also noted that at GPL values larger than 60%, the corresponding
415 cumulative frequencies are almost the same for both sets.

416

417

418 **3.3. New MFHW sets using a New Sampling approach, Latin hypercube sampling**

419 **(LHS)**

420 In previous sets, the full factorial linear experimental design was used to study the cleanup
421 efficiency. Using the FFS approach takes a relatively long CPU time to conduct a large
422 number of simulation runs (i.e. 4096 runs for each set). Introducing more complexity to the
423 models made the CPU time even longer. In order to decrease the required number of runs and
424 reduce the CPU time, Latin Hypercube Sampling (LHS) method was adopted. It should be
425 highlighted that the RSM fitted to results based on the FFS is linear whereas that fitted based
426 on LHS could be either linear or quadratic, which increases the accuracy of the fitted RSMs.
427 For these simulations, the Multiple Realization Optimizer (MEPO) software has been used to
428 link different stages of the simulations conducted using ECLIPSE100 automatically and to
429 perform pre and post-processing stages. MEPO (Schlumberger, 2013) is a software to
430 design, perform and post-process many simulations' runs in different simulation engines.
431 MEPO utilises powerful run management and provides faster results more efficiently. MEPO
432 utilises Python script to perform the pre and post-processing stages. Hence a new computer
433 code using the Python Programming Language (Python Software Foundation, 2013) was also
434 developed. MFHW Nf7 L600m base reference sets with different run numbers were
435 conducted and analysed to obtain the minimum (optimum) number of runs required for the
436 LHS approach.

437 The results of this new approach with LHS MFHWs with the original MFHW base
438 reference set were compared. The results indicated that using LHS, with fewer run numbers,
439 retained the main trends in tornado charts whilst reducing CPU time. It also ensures
440 achieving more accurate predictions for GPLs using both fitted linear and quadratic response

441 methods as it will be shown in section 3.4.1. Finally, the different number of runs for LHS
442 were compared to obtain the minimum number of runs with a reasonable error.

443

444 **3.3.1. Latin Hypercube Sampling (LHS)**

445 McKay *et al.* (1979) were the first to introduce Latin hypercube sampling (LHS). As a
446 mathematical and statistical method, LHS creates a sample of possible groups of variable
447 quantities. The LHS method is widely used to reduce the number of runs and CPU time. LHS
448 is based on optional dimensions' numbers, by which each sample is unique in each axis-
449 aligned hyperplane.

450 In this approach and during the creation of a sample collection of a function of n
451 parameters, the variation range of each parameter is divided into m intervals in which their
452 probability are equal. M sample points are then located in m intervals to satisfy the conditions
453 of the Latin hypercube. This equally spaced interval sampling technique is the key advantage
454 of LHS sampling compared to other sampling approaches. Another benefit of LHS is that
455 random samples can be taken one at a time, while it remembers what samples have been
456 taken up to now.

457

458 **3.3.2. MEPO Multiple Realization Optimizer**

459 MEPO (Schlumberger, 2013) was used in this study because this software enables the user
460 to choose between different sampling approaches, i.e., Latin Hypercube, full factorial design,
461 fractional factorial, Plackett-Burman and OVAT. On the other hand, In order to conduct the
462 LHS approach, the MEPO software was used. MEPO is a suitable software to design,
463 perform and post-process many simulation runs in different simulation engines. The MEPO
464 multiple realisation optimiser utilises a robust run management arrangement and allows the
465 user to attain faster results with relative ease.

466 In the previous MATLAB code, the results for each simulation run were read and exported
467 to an excel file (or a text-file) for each run, i.e., in addition to the simulation run done by
468 Eclipse, pre and post-processing were performed at the end of each run by MATLAB.
469 However, in MEPO, the results are stored, and at the end, the results of all runs could be
470 exported once into an excel-file. Additionally, the post-processing stage is faster using
471 MEPO, and this also results in less CPU time compared to the previous MATLAB code.

472

473

474 3.3.3. Python Programming Code

475 Python (Python Software Foundation, 2013) has been used in this study since MEPO
476 performs pre- and post-processing using Python scripts. Hence, a new Python code has been
477 developed to generate include-files for each run. Python is an excellent language for
478 programming, which has effective complex data structures and a simple but efficient tactic to
479 object-oriented programming. Python's stylish syntax and dynamic typing make it an
480 impeccable language for scripting and swift application development in many subjects on
481 most platforms. The Python interpreter also allows it to be implemented in C or C++ or other
482 languages callable from C.

483

484 3.4. New MFHW sets Using MEPO and LHS (MFHW-Sets 23 to 29 Nf7 L600m & Base 485 Reference Set)

486 In this section, the results of MFHW Nf7L600m base reference set (i.e. MFHW-Set 8) re-
487 run with different run numbers using the LHS approach are discussed. The first aim for
488 running MFHW Nf7L600m base reference set using LHS was to conduct a sensitivity
489 analysis on run numbers and to decrease the required number of runs and consequently to
490 reduce the CPU time. The second aim was to increase the accuracy of the fitted response
491 surface models. MFHW Nf7L600m base reference set was conducted with different run
492 numbers of 4096, 3000, 2000, 1000, 500, 250 and 100 using the LHS approach. Here, the
493 results of these sets and those of the original two-level full factorial MFHW Nf7L600m base
494 reference set are analysed and compared with each other, and a comprehensive error analysis
495 is conducted to obtain the optimum (minimum) required number of runs. Finally based on the
496 error analysis, the most accurate response surface model (full quadratic surface model) is
497 selected. For the new MFHW sets, which are based on the LHS experimental design
498 approach, in order to have a consistent assessment with results reported previously, the
499 impact of individual parameters in the tornado charts, are still studied based on the linear
500 surface model without interaction.

501 Here the tornado chart of MFHW-set 23 Nf7 L600m Base Reference set using LHS with
502 4096 run numbers (Figure 11) with that of the two-level full factorial sampling (FFS)
503 MFHW-Set 8 Nf7 L600m Base Reference set (Figure 10) with the only difference being
504 different sampling approaches is compared. The same trend is observed in both tornado

505 charts for all pertinent parameters. This observation ensures that changing the sampling
506 approach from two-level FFS design to LHS retained the main trends in tornado charts.

507 Comparing the tornado chart of MFHW Nf7 L600m Base Reference Set -Sets 23, 24, 25,
508 26, 27, 28 and 29, with different run numbers of 4096, 3000, 2000, 1000, 500, 250 and 100
509 respectively, with each other with the only difference being reducing run numbers from 4096
510 to 100 runs indicated that the same trend and values were observed in all tornado charts for
511 all pertinent parameters. These results indicate that by using LHS and reduction of run
512 numbers, the main trends in tornado charts has been retained whilst reducing CPU time.

513 Figure 12 shows the GPL accumulative frequency for seven different sets with different
514 run numbers (MFHW-Set23 to MFHW-Set29). Almost the same clean-up efficiency is
515 observed for all run numbers. However, it is noted that as the run numbers are decreased
516 (below 500), the curves obtained are not as smooth as those obtained with larger run numbers
517 (Figure 12 and Figure 13), this suggests that decreasing run numbers to values of 250 and 100
518 could not result in consistent histogram charts.

519 At this stage, in order to obtain the optimum (minimum) required number of runs as well
520 as the best response surface model to predict GPL values, a comprehensive error analysis was
521 conducted as described in the next section.

522

523 3.4.1. Error Analysis of Fitted Linear Response Surface Method

524 One of the main reasons for conducting the MFHW set with different run numbers using
525 LHS approach was to evaluate the level of improvement in the predictive capability of the
526 fitted surface functions compared to those fitted to that using the two-level FFS technique.
527 For this purpose, the errors of predicted GPL values of the MFHW with different run
528 numbers (run numbers of 4096, 3000, 2000, 1000, 500, 250 and 100) using ILRSM and those
529 of the relevant two-level FFS MFHW set were compared.

530 The root means square error, RMSE, Equation 7 and relative RMSE %, Equation 8, were
531 used to compare the results which are presented in Table 5.

$$532 \text{ RMSE} = \sqrt{\frac{\sum_{i=1}^n [\text{GPL}_{\text{predict}} - \text{GPL}_{\text{sim}}]^2}{n}} \quad 7$$

$$\text{relative RMSE}\% = \frac{\text{RMSE}_i - \text{RMSE}_{\text{run number of 4096}}}{\text{RMSE}_{\text{run number of 4096}}} * 100 \quad 8$$

533 Table 6 list the RMSE and also relative RMSE% for different run numbers using LHS and
 534 FFS. It is noted in Table 6 that IRSMs fitted to MFHW set using LHS approach with different
 535 run numbers predict GPL results more accurately than the relevant ILRSM using two-level
 536 FFS (except for LHS with run number 100). This observation suggests that generally,
 537 ILRSMs fitted to LHS runs predict GPLs better compared to those GPLs predicted by
 538 ILRSMs fitted to the data obtained using two-level FFS.

539 Figure 14 shows RMSE of ILRSMs versus run numbers for MFHW Nf7 L600m Base
 540 Reference sets with different sampling approaches, i.e., LHS, and two-level FFS. From
 541 Figure 14 in addition to the observation of having more accurate results for LHS runs, it is
 542 also noted that as the run numbers are decreased (below 1000), there is a significant increase
 543 in RMSE at all three production stages. This observation suggests that decreasing run
 544 numbers to values less than 500 (i.e., 250 and 100) result in less accurate ILRSMs and
 545 consequently higher RMSEs compared to larger run numbers. This finding is in agreement
 546 with what was formerly indicated in histogram charts, i.e., decreasing run numbers to the
 547 value of 250 and 100 resulted in less consistent charts than the ones for larger run numbers.
 548 Therefore, based on these results 1000 is considered the optimum number of runs.

549

550 **3.4.2. Error Analysis of Pure and Full Quadratic Response Surface Models**

551 The main reason to conduct this error analysis for different run numbers using LHS
 552 approach in addition to that presented in the previous section is to investigate the accuracy of
 553 pure quadratic response surface models (PQRSM), and full quadratic response surface
 554 models (FQRSM) fitted to LHS results.

555 In order to evaluate the reliability of these two models, the RMSE and relative RMSE of
 556 predicted GPL values of the MFHW set with different run numbers (run numbers of 4096,
 557 3000, 2000, 1000, 500, 250 and 100) using fitted PQRSM and FQRSM have been calculated.

558 Table 6 and Table 7 show RMSE and relative RMSE% of PQRSMs and FQRSMs fitted to
 559 the results of MFHW set using LHS approach with different run numbers. It is noted that the
 560 error of the predicted GPL values by FQRSM fitted to GPL values are less than the relevant
 561 ones for the predicted GPL values by PQRSM. In other words, the fitted FQRSMs predict the
 562 GPL values more accurately than the fitted PQRSMs except for the set with 100 run numbers.
 563 For this latter case, more significant errors in predicted GPL values by FQRSMs compared to
 564 the same GPL values predicted by PQRSMs is observed. That is because for FQRSMs, 91
 565 surface model coefficients are calculated based on just 100 data points whereas, for

566 PQRSMs, just 25 surface model coefficients are calculated based on the same 100 data
 567 points, therefore using 100 as the number of data points to fix a large number of the
 568 FQRSMs' coefficients is not desirable. These results confirm that FQRSM with a larger
 569 number of coefficients predict GPL more accurately if the number of data points is larger
 570 than 100.

571 Figure 15 show RMSE of ILRSM, PQRSM and FQRSM models versus run numbers for
 572 MFHW Nf7 L600m Base Reference sets with different sampling approaches, i.e., LHS and
 573 two-level FFS. From Figure 15 it is noted that the two-level FFS design is the least accurate
 574 sampling design and FQRSM is the most accurate design. It also indicates that the accuracy
 575 of the models with interaction terms (i.e. ILRSMs and FQRSMs with 79 and 91 coefficients,
 576 respectively) decreases significantly in small run numbers (i.e., 100 and 250) due to very few
 577 data points.

578 These results suggest that generally, LHS approach is a more realistic and reliable
 579 approach compare to two-level FFS design. Using LHS with optimum run numbers compared
 580 to two-level FFS sets reduces the CPU time significantly. The response surface model which
 581 best-predicted GPL values was FQRSM; in other words, FQRSM best describes the real
 582 physics of clean-up performance. The optimum (minimum) required a number of MFHW-
 583 Nf7L600 runs for FQRSMs was 1000 run numbers. Consequently, in the following
 584 simulation sets, LHS approach was used to increase the accuracy of the simulation while
 585 decreasing the CPU time.

586

587 **3.5. Impact of Number of Hydraulic Fractures**

588 **3.5.1. Fixed horizontal well length**

589 In this section, the results of MFHW-Set 1, MFHW-Set 8, MFHW-Set 12 and MFHW-Set
 590 13 with three, seven, nine and thirteen fractures placed on the same horizontal length of 600
 591 m respectively are discussed to evaluate the effect of fracture spacing. In these sets, the
 592 fracture spacing decreased from 300 in MFHW-Set 1 to 100, 75 and 50 m in MFHW-Set8
 593 (MFHW Nf7 L600 set), MFHW-Set12 (MFHW Nf9 L600 set) and MFHW-Set13 (MFHW
 594 Nf13 L600 set) respectively. For these sets, new models were set-up, and the Python code
 595 was modified accordingly.

596 Comparing the tornado chart of MFHW-Set1 (Figure 4) and those of these new MFHW
 597 sets, i.e. MFHW Nf7 L600 set (Figure 11), MFHW Nf9 L600 sets (Figure 16) and MFHW
 598 Nf13 L600 set (Figure 17), it is observed that the trend and magnitude of effect of all

599 parameters are almost alike indicating that fracture spacing does not affect the cleanup
 600 efficiency of MFHWs. This similarity is extended to the effect of k_m . That is, in all MFHW
 601 sets, with a different number of fractures (Nfs) and thereby different FF injected volume, the
 602 effect of k_m on Pc is still more dominant than that on fluid flow.

603 Figure 18 shows the swiftness of cleanup operation for the following sets, MFHW-Set1
 604 (MFHW Nf3 L600), MFHW-Set8 (MFHW Nf7 L600), MFHW-Set12 (MFHW Nf9 L600)
 605 and MFHW-Set13 (MFHW Nf13 L600). It is noted that generally minimal differences are
 606 observed when changing Nf from 3 to 13. This observation again reconfirms that the change
 607 in fracture spacing does not affect the cleanup efficiency of MFHWs.

608

609 3.5.2. Fixed Fracture spacing

610 A new model was set-up with ten 90 m fractures placed on the 900 m horizontal well
 611 length to capture the impact of horizontal well length on the cleanup efficiency of MFHWs
 612 when fracture spacing is the same. Here, the fracture spacing is the same as the one for
 613 MFHW-Set8 (MFHW Nf7 L600 set) but with longer horizontal length to accommodate ten
 614 fractures.

615 Comparing the tornado chart for MFHW-Set8, Figure 11, with that of MFHW-Set 14,
 616 Figure 19, shows a similar trend and values for coefficients of different parameters for these
 617 cases. Minimal differences are noted between MFHW-Set8 (MFHW Nf7 L600 and MFHW-
 618 Set14 (MFHW Nf10 L900) in Figure 20. These results confirm that the impact of the number
 619 of fractures on the cleanup efficiency, even when the fracture spacing is the same, is small. It
 620 should be noted that for any of these sets the amount of gas production is different
 621 highlighting the impact of the number of fractures on production. However, the GPL ratio
 622 seems to be the same

623

624 3.6. Increased FVR MFHW-Set 2

625 In MFHW-Set 2, the fracture volume ratio has been raised from 2 in the MFHW-set1 to 5.
 626 Once the tornado chart of MFHW-Set 2, Figure 21a, is compared with that of MFHW-Set 1
 627 (FVR=2) with the only difference being a higher FVR for MFHW-Set 2, Figure 4, It is
 628 observed that the trends are more or less the same.

629 The k_f in both cases has the most substantial effect on GPL, and the sequences of the
 630 significance of other parameters are reasonably similar. If the high FVR MFHW set is
 631 compared with the relevant set in vertical well sets, i.e., VW-Set 9, the same trend is

632 observed for all parameters except for k_m , which has been discussed earlier (Figure 21b). It is
633 also noted that Pc pertinent parameters are more critical in the MFHW set whilst endpoints
634 and exponents of Corey type relative permeability curves for gas and FF in both matrix and
635 frack are more critical in the VW set. These observations are due to the fact that FF
636 production has a more detrimental effect on gas production in the MFHW set due to smaller
637 area perpendicular to flow at the wellbore (also known as near wellbore choking effect).
638 Hence for the MFHW set the effect of flow from the matrix towards fracture during the
639 backflow clean-up is less important and rather imbibition of fracture fluid governed by matrix
640 capillary pressure, which depends on k_m is more important. This trend was observed for all
641 MFHW sets presented in this exercise.

642 Similar to what was reported previously (Nasriani and Jamiolahmady, 2018a) for the VW
643 sets, faster clean-up is observed for the MFHW base reference set compared to the MFHW
644 FVR=5. This observation is due to less FF injected in the MFHW base reference set, which
645 requires less time to clean.

646

647 **3.7. Extended ST MFHW-Set 3**

648 In MFHW-Set 3, the soaking time (ST) has been extended from 2 days in the MFHW-set1
649 to 20 days. Considering the impact of the 12 parameters in two sets of MFHW-Set 3 (ST=20)
650 and MFHW-Set 1 (ST=2) with the only difference being a longer soaking time for MFHW-
651 Set 3), the same observation is noted as that of (Nasriani and Jamiolahmady, 2018a) for VW
652 sets, i.e., the observed magnitude and trends of all pertinent parameters are more or less the
653 same. However, the absolute value of Pc Pertinent parameters, i.e. IFT and λ , are larger than
654 those of MFHW-Set 1, confirming the observation reported for the VW sets that extending
655 soaking time makes the impact of Pc on production loss to be more significant (Nasriani and
656 Jamiolahmady, 2018a).

657 Faster clean-up was observed for the extended ST MFHW set compared to the MFHW
658 base reference set, but only at early production times, the same observation as the one
659 observed for VWs (Nasriani and Jamiolahmady, 2018a).

660

661 **3.8. Tighter Formations by a Factor of 10 and 100 MFHW-Sets 4 & 7**

662 In this section, the variation range corresponding to k_m has been reduced from 1 μ D-100
663 μ D in the MFHW-set 1 to 0.1 μ D-10 μ D and 0.01 μ D-1 μ D in MFHW-Sets 4 & 7
664 respectively.

665 If the tornado charts of MFHW-Set 4 (KMR=10), Figure 22, is compared with that of
666 MFHW-Set 1 (KMR=1) with ten times tighter formation for MFHW-Sets 4, Figure 4, it is
667 noted that the observed trends are the same except for the k_m coefficient. That is, in this
668 MFHW-Set with the tighter formation, the first effect of k_m on GPL (i.e. a rise in matrix
669 permeability that advances fluid mobility and lessens GPL) is dominant whilst in MFHW-Set
670 1 the second effect (i.e. a rise in k_m that decreases Pc and raises GPL) was dominant. Since in
671 this tighter set, i.e., MFHW-Set 4, the k_m range has been reduced by a factor of 10, Pc is
672 already high enough, and hence the impact of k_m on mobility is more significant.

673 If MFHW-Set 4 is compared with the corresponding VW set, VW-Set 4, the same
674 observation as that highlighted in previous sets, is noted.

675 When the tornado chart of MFHW-Set 7 (KMR=100), Figure 23, is compared with that of
676 MFHW-Set 1 (KMR=1), Figure 4, it is observed that the trends of impact of all parameters
677 are the same except for the k_m and IFT coefficients. In this very tight formation, the first
678 effect of k_m on GPL (i.e. if k_m increases that results in an improvement in the mobility of the
679 fluid and consequently reduction in GPL) is dominant. Conversely, in MFHW-Set 1 the
680 second effect (i.e. if k_m increases that decreases Pc and accordingly an increase in GPL) is
681 dominant. This is the same observation as that in MFHW-Set 4 with k_m range decreased by a
682 factor of 10. Since in the current MFHW-Set 7, the range of k_m has been decreased 100 times
683 smaller; now it is significantly more difficult for fluid to flow in the matrix; hence the effect
684 of k_m on mobility is more important. Figure 23 shows that the value of the k_m coefficient is
685 almost -1 at all production periods (in MFHW-Set 4, Figure 22, the value of k_m was almost -
686 0.1) indicating that as the formation gets tighter the first effect of k_m on GPL is most
687 pronounced.

688 It is noted that in MFHW-Sets 7, the IFT coefficient trend changes as production time
689 increases. This highlights that using IFT reducing agent could improve the cleanup
690 efficiency. This observation will be discussed in details in Section 3.8, 3.9 & 3.10.

691 Slower clean-up was observed for the tighter formations MFHW-Set 4 & 7 (MFHW with
692 KMR=10 & 100) compared to the MFHW-set1 using histogram charts. It shows the same
693 observation similar to what was reported previously for the VW sets (Nasriani and
694 Jamiolahmady, 2018a).

695
696

3.9. MFHW-Sets with different DP values

697 In this section, DP has been changed from the default value in MFHW base reference set
698 (1000 psi) to 100 and 4000 psi in MFHW-Sets 5 & 6 respectively.

699 Considering the impact of the 12 parameters in two sets of MFHW-Set 5 (DP=100),
700 Figure 24, and that of MFHW-Set 1 (DP=1000) with the only difference being a lower DP by
701 a factor of 10 for MFHW-Set 5, Figure 4, it is interesting to note that the observed trends of
702 pertinent parameters are the same with the exception of an increase in the absolute value of
703 P_c pertinent parameters. This observation is in line with what was reported previously for low
704 DP VW sets, i.e., in low DP sets the influence of P_c on GPL is more pronounced (Nasriani
705 and Jamiolahmady, 2018a).

706 In MFHW-Set 5, the impact of the endpoints and exponents of Corey type relative
707 permeability curves for the fluid in the porous medium of the rock is more important than that
708 of these parameters in MFHW-Set 1 confirming the observation noted in the corresponding
709 VW sets. That is, in low DP sets, it is more important how fluid (Gas and FF) flows from the
710 matrix to fracture than how it flows from fracture to the wellbore. Figure 24 shows a small
711 negative value for the k_m coefficient after ten days indicating that at this period the effect of
712 k_m on GPL is minimal, but due to its negative sign, it could be concluded that the first
713 influence of k_m on production loss is more dominant.

714 In MFHW-Set 6, DP was increased 4 times larger (4000psi) than its base value (1000psi).
715 When the results of these two sets were compared it was observed that the trends of pertinent
716 parameters are more or less similar except for a drop in the magnitude of P_c pertinent
717 parameters. This observation is in line with what was reported previously for high DP VW
718 sets, i.e., in high DP sets the weight of P_c on production improvement was less pronounced
719 (Nasriani and Jamiolahmady, 2018b; Nasriani *et al.*, 2018).

720 The impact of the endpoints and exponents of Corey type relative permeability curves for
721 fluid in the matrix was also less distinct than that of these parameters in MFHW-Set 1, this
722 confirms the observation noted in the VW sets, that is, in high DP sets it is less important
723 how fluid (Gas and FF) flows from the matrix to fracture than how it flows from fracture to
724 the wellbore. This follows the same trend as what was observed above for the low DP set,
725 MFHW DP=100 (MFHW-Set 5). Slower/faster clean-up was observed for this lower/higher
726 DP set compared to the MFHW base reference set.

727

728 3.10. MFHW-Sets with Nf7 and L600m with different k_m ranges

729 Following the IFT trend change which was observed in Section 3.8 for MFHW-Set 7 with
730 three fractures, three different MFHW-Sets (with Nf=7 rather than sets with Nf=3 discussed
731 in section 3.8) with different k_m ranges were studied. For this purpose, the range of k_m was
732 dropped from 1 μD -100 μD in the MFHW-Set8 Nf7 L600 base reference set to 0.1 μD -10 μD
733 and 0.01 μD -1 μD in MFHW-Set9 and MFHW-Set10, respectively.

734 Analysis of the impact of the 12 parameters in three sets of MFHW-Set 8 (KMR=1),
735 Figure 11, MFHW-Set9 (KMR=10), Figure 26, and MFHW-Set10 (KMR=100), Figure 27 ,
736 shows that the trends of most of the parameters are more or less the same, including the trend
737 of the k_m coefficient. However, in MFHW-Set10, k_m is the most critical parameter at 30 and
738 370 days and the second most crucial parameter after k_f at ten days. That is because, in the
739 current set, MFHW-Set10, k_m range has been reduced by a factor of 100, the mobility of
740 different fluids in the matrix becomes very vital. If one compares the fluid mobility pertinent
741 parameters in MFHW-Set8, MFHW-Set9 and MFHW-Set10, it is noted that fluid mobility
742 within the matrix of the rock is more/most significant in tighter/tightest formations
743 (KMR=10/ KMR=100), i.e., the tighter the formation, the more important the effect of fluid
744 mobility on clean-up efficiency.

745 From the data of Figure 27, it is also observed that the trend of IFT coefficient has
746 changed from negative in MFHW-Set 8 (KMR=1) and MFHW-Set9 (KMR=10) to positive in
747 the tightest set (MFHW-Set10 (KMR=100)). Since this trend change of IFT could have an
748 impact on P_c , therefore it is essential to study the impact of P_c on the cleanup performance in
749 this section for these three MFHW-Sets. Capillary pressure of these three MFHW-Sets was
750 calculated by choosing the corresponding values of IFT, k_m and λ for the worst (maximum
751 GPL) and best (Minimum GPL) case scenarios from the corresponding tornado charts in
752 addition to Equations 1 and 2. The calculated P_c data for these three MFHW-Sets shows that
753 in this set, MFHW-Set10, the magnitude of the P_c value for the worst case is considerably
754 larger than that of the best case whereas, in MFHW-Set8 and MFHW-Set9, the P_c value of
755 the best case is higher than that of the worst case. This observation highlights that in MFHW-
756 set 8 and MFHW-set-9, it is recommended to retain the FF within the matrix employing
757 higher capillary pressure, however in the tightest formation set, MFHW-Set10, it is
758 recommended to flowback the FF as much as possible and minimise the FF saturation in the
759 matrix. This is attributed to very tight nature of the formation (in MFHW-Set10) in which

760 keeping the FF in the matrix has a more harmful impact on production than its adverse effect
 761 once it is produced through the fracture.

762 Figure 28 shows P_c versus water saturation, S_w , for those sets above (MFHW-Set8,
 763 MFHW-Set9 and MFHW-Set10). It is demonstrated that higher P_c values were observed for
 764 the best case than the worst case at all water saturation values in Sets MFHW-Set8 and
 765 MFHW-Set9 (indicating that keeping FF in the matrix is better and results in less GPL).
 766 Conversely, higher P_c values were observed in MFHW-Set10 for the worst case than the best
 767 case at all water saturation values (it is best to reproduce the injected FF from the matrix). In
 768 other words, in MFHW-Set 10, contrasting the previous two sets, using chemicals agents to
 769 reduce IFT and consequently decreasing P_c could lessen GPL.

770 According to the results of these three sets (MFHW-Set 8, MFHW-Set 9 and MFHW-Set
 771 10), matrix permeability plays a vital role in hydraulic fracturing design. For those sets with
 772 k_m variation 1 μD -100 μD and 0.1 μD -10 μD , using IFT reducing agents will have a
 773 detrimental impact on the production and consequently increases GPL. Conversely, in very
 774 tight sets with matrix permeability variation 0.01 μD -1 μD , it is recommended to use IFT
 775 reducing agents in order to decrease P_c and consequently reduce GPL.

776 All these runs were at moderate DP of 1000 psi. In order to confirm that this observation is
 777 also valid at low and high DP values, six new MFHW-Sets were conducted.

778 Three new sets (MFHW-Set15 Nf7-L600m DP4000, MFHW-Set17 Nf7-L600m KMR10
 779 DP4000 and MFHW-Set19 Nf7-L600m KMR100 DP4000) were conducted to capture the
 780 effect of k_m at high DP=4000 psi. The k_m range is 1 μD -100 μD in MFHW-Set15, 0.1 μD -10
 781 μD in MFHW-Set17 and 0.01 μD -1 μD MFHW-Set19 with DP=4000 psi in all of these sets.

782 A comparison of the tornado charts of these sets, Figure 29, Figure 30 and Figure 31,
 783 shows that k_f is the most important parameter affecting GPL for all three sets at all production
 784 periods. Other fluid mobility parameters in the fracture (k_{maxwf} , k_{maxwf} , n_{wf} and n_{gf}) are the
 785 second most important set of parameters affecting GPL for MFHW-set15 and MFHW-set17
 786 at all production periods and the third most important parameter for MFHW-set19. As the k_m
 787 variation range is 10 and 100 time reduced in MFHW-set17 and MFHW-set19, the impact of
 788 k_m and fluid mobility in the matrix become progressively more important. This is because, in
 789 tighter (tightest) formation, the fluid flow through the matrix becomes more (most)
 790 challenging.

791 Figure 31 shows that the trend of IFT has changed in MFHW-set19 compared to the other
 792 two sets. In order to fully understand the effect of P_c in these sets, the same approach as the

793 one conducted for the three previous sets, i.e., MFHW-set8, 9 & 10, was followed by
794 preparing the corresponding Pc values versus Sw for the best/worst scenarios, Figure 32.
795 Data in this Figure confirms that for those sets with KMR of 1 and 10, having higher Pc,
796 corresponding to the best case scenario, is more favourable and application of IFT reducing
797 agents will increase GPL. Contrariwise, whilst in the very tight set (KMR=100) with higher
798 Pc for the best case scenario, it is recommended to use such chemicals in order to diminish Pc
799 and consequently minimise GPL.

800 Following the results of the previous sets with moderate and high DP, here in MFHW-Sets
801 11, 16 and 18, DP was lowered by a factor of 10 to 100 psi. Here, the k_m range is 1 μD -100
802 μD in the MFHW-Set11, 0.1 μD -10 μD in MFHW-Set16 and 0.01 μD -1 μD MFHW-Set18
803 with DP=100 psi in all of these sets.

804 The tornado charts of these three low DP sets, i.e., Figure 33, Figure 34 and Figure 35, and
805 their Pc plots versus Sw for the best/worst cases of these sets (Figure 36) show the same
806 results as the ones observed in high and moderate DP.

807 Comparing the results of all 9 sets (with different DPs and K_m ranges) confirms that
808 regardless of DP, for those MFHW sets with k_m ranges of 1 μD -100 μD and 0.1 μD -10 μD ,
809 the application of IFT reducing agents will raise GPL whilst in very tight sets with the k_m
810 range of 0.01 μD -1 μD it is recommended to use such additives to diminish Pc and
811 consequently minimize GPL. Specifically, it is best to retain FF in the matrix in sets with k_m
812 ranges of 1 μD -100 μD and 0.1 μD -10 μD . However, the positive effect of retaining FF in the
813 matrix weakens in sets with the k_m range of 0.1 μD -10 μD compared to the sets with the k_m
814 range of 1 μD -100 μD . In fact, in sets with the tightest formations, i.e., k_m range of 0.01 μD -1
815 μD , this trend becomes opposite, i.e., it is best to backflow the FF. In other words, it is
816 observed that using IFT reducing agents as an additive in fracturing fluid is not recommended
817 for tight formations (it reduces the gas production rate) whilst it is highly recommended to
818 use such agents for ultratight formations (it enhances the gas production rate).

819 If the tornado charts of the three low DP sets (Figure 33, Figure 34 and Figure 35) are
820 compared with the relevant high DP sets (Figure 29, Figure 30 and Figure 31), it is noted that
821 fluid mobility pertinent parameters (k_{maxgm} , n_{gm} , k_{maxwm} and n_{wm}) in the matrix are more
822 important at low DP sets compared to the relevant ones in high DP sets. This is because as
823 DP decreases, fluid mobility within the matrix becomes more critical and consequently have
824 a more significant impact on the GPL reduction.

825

826 4. Conclusions

827 Following the extensive investigation on clean-up efficiency of VWs, this study has
828 extended the previous work (Nasriani et al., 2018; Nasriani and Jamiolahmady, 2018a) to
829 MFHWs systems.

830 A summary of the main conclusions is given below:

- 831 1. The results of VW and MFHW base reference sets which had similar properties were
832 compared.
 - 833 a. The k_m trend in the MFHW base reference set was different from that in
834 the VW Set. It was shown that this k_m trend change (from having a negative
835 to a positive coefficient value) in the MFHW set was due to the flow
836 geometry change and how the well was completed.
 - 837 b. It was noted that P_c pertinent parameters were more important in the
838 MFHW sets whilst endpoints and exponents of Corey type relative
839 permeability curves for gas and FF in both matrix and the fracture were
840 more important in the VW sets.
 - 841 i. This observation suggests that FF production had a more
842 detrimental effect on gas production in the MFHW set. In other
843 words, having a higher P_c that results in more FF to be further
844 imbibed into the matrix and less resistance to the gas flow, is
845 more important in MFHWs.
 - 846 c. Faster clean-up was observed for MFHW compared to VW. This was due to
847 having a higher production rate in MFHW sets.
 - 848 d. In Reduced (increased) DP MFHW sets, slower (faster) clean-up was
849 observed; this is similar to what was previously reported for the
850 corresponding VW sets
- 851 2. In the reduced matrix permeability range MFHW sets, the first effect of k_m on GPL (i.e.
852 a rise in k_m increasing the fluid mobility and diminishing GPL) was dominant (i.e. k_m
853 coefficient was negative). Conversely, in MFHW-Set 1 (MFHW base reference set) the
854 second effect (i.e. a rise in k_m value, diminishing P_c and escalate GPL) was dominant
855 (i.e. positive k_m coefficient).
- 856 3. In low (high) DP MFHW sets, P_c has a stronger (weaker) impact on GPL. This trend is
857 similar to what was previously reported for the corresponding low (high) DP VW sets.

- 858 4. Increasing horizontal well length while the fracture spacing was fixed did not change
859 the fracture clean-up efficiency at all.
- 860 5. Slower clean-up is observed for the tight and ultratight formations compared to the base
861 reference set due to a lower production rate of the tightest (and tighter) formation
862 resulting in a slower and less efficient clean-up.
- 863 6. Regardless of pressure drop, for the MFHW sets with matrix permeability variation
864 ranges of 1 μD -100 μD and 0.1 μD -10 μD , the application of the IFT reducing agents
865 will intensify GPL whilst in ultratight sets (i.e., k_m range of 0.01 μD -1 μD), it is
866 recommended to use such chemicals to weaken P_c and consequently diminish GPL.
- 867 a. In other words, it is concluded that using IFT reducing agents as an additive in
868 fracturing fluid is not recommended for tight formations (it reduces the gas
869 production rate) whilst it is highly recommended for ultratight formations (it
870 enhances the gas production rate).
- 871 7. Although the impact of fracture interference/fracture spacing on flow is significant, its
872 impact on clean-up performance is minimal in MFHWs systems with different fracture
873 spacing.
- 874 8. In this study, a new sampling approach (Latin Hypercube Sampling (LHS) method) is
875 introduced and the results were compared with the full factorial sampling approach.
- 876 a. The results of MFHW sets with LHS suggest that generally, LHS approach is a
877 more realistic and reliable sampling approach compared to the two-level FFS
878 experimental design.
- 879 b. Using LHS with an optimum run number (1000 run numbers) reduces the CPU
880 time significantly compared to two-level FFS sets.
- 881 c. The response surface model, which best-predicted GPL values was FQRSM. In
882 other words, FQRSM describes the real physics of clean-up performance better.
- 883
- 884

885 Acknowledgements

886 The above study was conducted as a part of the Gas-condensate Recovery Project at Heriot-
887 Watt University. This research project is sponsored by Daikin, DongEnergy,
888 Ecopetrol/Equion, ExxonMobil, GDF, INPEX, JX-Nippon, Petrobras, RWE, Saudi-Aramco
889 and TOTAL, whose contribution is gratefully acknowledged.

890

891 Nomenclature

892 k absolute reservoir permeability
893 k_{max} end point of the Corey relative permeability formula
894 P pressure
895 P_c capillary pressure
896 S saturation
897 n exponent of the Corey relative permeability formula
898 x x-direction
899 y y-direction
900 z z-direction

901

902 Subscript

903 g gas
904 w water
905 r residual
906 f fracture
907 m matrix

908 Abbreviations

909 CPU Central Processing Unit
910 DP Pressure drawdown
911 FF fracture fluid
912 FFS full factorial sampling
913 FGPT total gas cumulative production
914 FVR the ratio of injected fracture fluid to fracture volume
915 FQRSM Full Quadratic Response Surface model
916 GPL gas production loss
917 HF Hydraulic Fracturing
918 ILRSM linear response surface model with interaction
919 IFT interfacial tension
920 KMR Matrix Permeability Ratio, i.e., if $KMR=10$ mean the k_m variation range is reduced by factor
921 of 10
922 LHS Latin Hypercube Sampling
923 LRSM linear response surface model
924 MEPO Multiple Realization Optimizer
925 MFHW Multiple Fractured Horizontal Well
926 PQRSM Pure Quadratic Response Surface model
927 RMSE The root means square error
928 RSM Response Surface Methodology
929 ST Shut-in/Soaking time
930 VW Vertical Well
931

932 **References**

- 933 Brooks, R.H., Corey, A.T., 1966. Properties of porous media affecting fluid flow. *J. Irrig.*
934 *Drain. Div.* 92, 61–90.
- 935 Brooks, R.H., Corey, A.T., 1964. Hydraulic properties of porous media.
- 936 Clark, J.B., 1949. A Hydraulic Process for Increasing the Productivity of Wells. *J. Pet.*
937 *Technol.* 1, 1–8. <https://doi.org/10.2118/949001-G>
- 938 Dong, Z., Holditch, S.A., McVay, D., Ayers, W.B., 2011. Global Unconventional Gas
939 Resource Assessments. <https://doi.org/10.2118/148365-MS>
- 940 Economides, M.J., Martin, A.N., 2010. How to decide between horizontal transverse,
941 horizontal longitudinal and vertical fractured completion, in: *Proceedings - SPE Annual*
942 *Technical Conference and Exhibition*. pp. 2474–2491.
- 943 Garrison, A.D., 1945. Treatment of wells.
- 944 Gdanski, R.D., Weaver, J., Slabaugh, B., Walters, H., Parker, M., 2005. SPE 94649 Fracture
945 Face Damage - It Matters. *Water*.
- 946 Ghahri, P., Jamiolahmady, M., Sohrabi, M., 2011. SPE 144114 A Thorough Investigation Of
947 Cleanup Efficiency Of Hydraulic Fractured Wells Using Response Surface
948 Methodology. <https://doi.org/10.2118/144114-MS>
- 949 Ghahri, P., Jamiolahmady, M., Sohrabi, M., 2009. Investigation of cleanup efficiency of
950 hydraulically fractured wells in gas condensate reservoirs, in: *8th European Formation*
951 *Damage Conference 2009 - New Technologies for Conventional and Unconventional*
952 *Reservoirs*. pp. 537–551.
- 953 Halliburton [WWW Document], 2018. . 125 W Missouri Midland, TX 79701. URL
954 [https://www.halliburton.com/en-US/ps/testing-subsea/reservoir-testing-](https://www.halliburton.com/en-US/ps/testing-subsea/reservoir-testing-analysis/calibr.html?node-id=i4msmulo)
955 [analysis/calibr.html?node-id=i4msmulo](https://www.halliburton.com/en-US/ps/testing-subsea/reservoir-testing-analysis/calibr.html?node-id=i4msmulo)
- 956 Height, B.C., 1944. Process of increasing permeability of sands and strata.
- 957 Holditch, S.A., 1979. Factors Affecting Water Blocking and Gas Flow From Hydraulically
958 Fractured Gas Wells. <https://doi.org/10.2118/7561-PA>
- 959 Jamiolahmady, M., Alajmi, E., Nasriani, H.R., Ghahri, P., Pichestapong, K., 2014. A
960 Thorough Investigation of Clean-up Efficiency of Hydraulic Fractured Wells Using
961 Statistical Approaches. *SPE Annu. Tech. Conf. Exhib.* 27-29 October.,
962 <https://doi.org/10.2118/170862-MS>
- 963 Jamiolahmady, M., Sohrabi, M., Ghahri, P., 2009. Investigation of Cleanup Efficiency of
964 Hydraulically Fractured Wells in Gas Condensate Reservoirs.

- 965 <https://doi.org/10.2118/121916-MS>
- 966 Lee, R.E., 1939. Method of treating a producing formation.
- 967 McKay, M.D., Beckman, R.J., Conover, W.J., 1979. A Comparison of Three Methods for
968 Selecting Values of Input Variables in the Analysis of Output from a Computer Code.
969 *Technometrics* 21, 239–245. <https://doi.org/10.2307/1268522>
- 970 Montgomery, K.T., Holditch, S.A., Berthelot, J.M., 1990. Effects of fracture fluid invasion
971 on cleanup behavior and pressure buildup analysis, in: *Proceedings - SPE Annual*
972 *Technical Conference and Exhibition*. pp. 279–290.
- 973 Nasriani, H.R., 2017. Cleanup efficiency of hydraulically fractured vertical and multiple
974 fractured horizontal wells. Heriot-Watt University.
- 975 Nasriani, H.R., Jamiolahmady, M., 2018a. Maximizing fracture productivity in
976 unconventional fields; analysis of post hydraulic fracturing flowback cleanup. *J. Nat.*
977 *Gas Sci. Eng.* 52. <https://doi.org/https://doi.org/10.1016/j.jngse.2018.01.045>
- 978 Nasriani, H.R., Jamiolahmady, M., 2018b. A Comparison of Clean-Up Efficiency of Multiple
979 Fractured Horizontal Wells and Hydraulically Fractured Vertical Wells in Tight Gas
980 Reservoirs, in: *SPE Europec Featured at 80th EAGE Conference and Exhibition*. Society
981 of Petroleum Engineers. <https://doi.org/10.2118/190862-MS>
- 982 Nasriani, H.R., Jamiolahmady, M., Alajmi, E., 2014a. An Integrated Study of Cleanup
983 Efficiency of Short Hydraulic Fractured Vertical Wells Using Response Surface
984 Methodology, in: *76th EAGE Conference and Exhibition 2014*.
985 <https://doi.org/10.3997/2214-4609.20141380>
- 986 Nasriani, H.R., Jamiolahmady, M., Alajmi, E., Ghahri, P., 2014b. A Study of Hydraulic
987 Fracturing Clean-up Efficiency in Unconventional Gas Reservoirs Using Statistical
988 Approaches, in: *ECMOR XIV-14th European Conference on the Mathematics of Oil*
989 *Recovery*.
- 990 Nasriani, H.R., Jamiolahmady, M., Saif, T., Sánchez, J., 2018. A systematic investigation into
991 the flowback cleanup of hydraulic-fractured wells in unconventional gas plays. *Int. J.*
992 *Coal Geol.* 193. <https://doi.org/10.1016/j.coal.2018.04.012>
- 993 Pope, D., Britt, L.K., Constien, V., Anderson, A., Leung, L., 1996. Field Study of Guar
994 Removal from Hydraulic Fractures. *SPE Int. Symp. Form. Damage Control* 1–7.
995 <https://doi.org/10.2118/31094-MS>
- 996 Python Software Foundation, 2013. Python Programming Language, Python v2.7.6. Python
997 Softw. Found.

- 998 Schlumberger, 2013. MEPO Multiple Realization Optimizer; MEPO4.2.0; Build:2617;
999 Date:2013-Apr-25_15-59. SPT Group; A Schlumberger Co.
- 1000 Tech-Flo Consulting [WWW Document], 2019. . Tech-Flo Consult. | 9701 Pozos Ln,
1001 Conroe, TX 77303 | 494-4330. URL <http://www.tech-flo.net/frac-flowback.html>
- 1002 The MathWorks, 2013. MATLAB and Statistics Toolbox Release 2014b (8.4.0.150421).
1003 Natick Inc.
- 1004 Thomas, L.K., Katz, D.L., Tek, M.R., 1968. Threshold pressure phenomena in porous media.
1005 Soc. Pet. Eng. J. 8, 174–184.
- 1006
- 1007
- 1008

1009 **5. Tables**

1010

Table 1 VW model

1011

$X_f(\text{m})$	$w_f(\text{m})$	$X_{\text{res}}(\text{m})$	$Y_{\text{res}}(\text{m})$	$Z_{\text{res}}(\text{m})$
100 or 400	0.004	2000	2000	40

1012

1013

1014

1015

Table 2 The parameters' variation range

Parameter	Min	Max
k_f (D)	1	30
k_m	1 μD	100 μD
λ	1	4
IFT (mNm/m)	2	50
n_{gm}	1.5	5
n_{wm}	1.2	4
k_{maxg}	0.5	1.0
k_{maxw}	0.05	0.6
n_{gf}	1.5	5
n_{wf}	1.2	4
k_{maxg}	0.5	1.0
k_{maxw}	0.1	0.75

1016

1017 Table 3a VW Set analysed

Set Name	DP (Psi)	FVR	Shut-in time (days)	Frack Length (m)	k_f (D)	k_m (μ D)	lam	IFT	η_{gm}	η_{wm}	k_{maxgm}	k_{maxwm}	η_{gf}	η_{wf}	k_{maxgf}	k_{maxwf}
Default Values	1000	2	2	400	1-30	1-100	1-4	2-50	1.5-5	1.2-4	0.5-1	0.05-0.6	1.5-5	1.2-4	0.5-1	0.1-0.75
VW-Set base reference set	✓	✓	✓	✓	✓	✓	✓	✓	✓	✓	✓	✓	✓	✓	✓	✓
VW-Set 9	✓	5	✓	✓	✓	✓	✓	✓	✓	✓	✓	✓	✓	✓	✓	✓
Y direction VW-Set	✓	✓	✓	✓	✓	✓	✓	✓	✓	✓	✓	✓	✓	✓	✓	✓

1018

1019

1020

1021

1022

Table 3b MFHW Set analysed

Set Name	No. of fracks	Horizontal Length (m)	DP (Psi)	FVR	Shut-in time (days)	k_f (D)	k_m (μ D)	λ_{am}	Sampling Approach	Number of Runs
Default Values	3	600	1000	2	2	1-30	1-100	1-4	FFS	4096
MFHW-Set 1 (base reference set)	✓	✓	✓	✓	✓	✓	✓	✓	✓	✓
MFHW-Set 2	✓	✓	✓	5	✓	✓	✓	✓	✓	✓
MFHW-Set 3	✓	✓	✓	✓	20	✓	✓	✓	✓	✓
MFHW-Set 4	✓	✓	✓	✓	✓	✓	0.1-10	✓	✓	✓
MFHW-Set 5	✓	✓	100	✓	✓	✓	✓	✓	✓	✓
MFHW-Set 6	✓	✓	4000	✓	✓	✓	✓	✓	✓	✓
MFHW-Set 7	✓	✓	✓	✓	✓	✓	0.01-1	✓	✓	✓
MFHW-Set 8	7	✓	✓	✓	✓	✓	✓	✓	✓	✓
MFHW-Set 9	7	✓	✓	✓	✓	✓	0.1-10	✓	✓	✓
MFHW-Set 10	7	✓	✓	✓	✓	✓	0.01-1	✓	✓	✓
MFHW-Set 11	7	✓	100	✓	✓	✓	✓	✓	✓	✓
MFHW-Set 12	9	✓	100	✓	✓	✓	✓	✓	✓	✓
MFHW-Set 13	13	✓	100	✓	✓	✓	✓	✓	✓	✓
MFHW-Set 14	10	900	100	✓	✓	✓	✓	✓	✓	✓
MFHW-Set 15	7	✓	4000	✓	✓	✓	✓	✓	✓	✓
MFHW-Set 16	7	✓	100	✓	✓	✓	0.1-10	✓	✓	✓
MFHW-Set 17	7	✓	4000	✓	✓	✓	0.1-10	✓	✓	✓
MFHW-Set 18	7	✓	100	✓	✓	✓	0.01-1	✓	✓	✓
MFHW-Set 19	7	✓	4000	✓	✓	✓	0.01-1	✓	✓	✓
MFHW-Set 20	7	✓	✓	✓	✓	✓	100-10000	✓	✓	✓
MFHW-Set 21	9	✓	✓	✓	✓	✓	100-10000	✓	✓	✓
MFHW-Set 22	13	✓	✓	✓	✓	✓	100-10000	✓	✓	✓
MFHW-Set 23	7	✓	✓	✓	✓	✓	✓	✓	LHS	✓
MFHW-Set 24	7	✓	✓	✓	✓	✓	✓	✓	LHS	3000
MFHW-Set 25	7	✓	✓	✓	✓	✓	✓	✓	LHS	2000
MFHW-Set 26	7	✓	✓	✓	✓	✓	✓	✓	LHS	1000
MFHW-Set 27	7	✓	✓	✓	✓	✓	✓	✓	LHS	500
MFHW-Set 28	7	✓	✓	✓	✓	✓	✓	✓	LHS	250
MFHW-Set 29	7	✓	✓	✓	✓	✓	✓	✓	LHS	100

1023

Table 4 Parameters of the worst / best scenarios for the Base Reference Set

No.	Parameter	Case	
		Worst	Best
1	k_f (D)	1	30
2	k_m (μ D)	1	100
3	λ	4	1
4	IFT (mNm/m)	2	50
5	n_{gm}	5	1.5
6	n_{wm}	4	1.2
7	k_{maxgm}	0.5	1.0
8	k_{maxwm}	0.05	0.6
9	n_{gf}	5	1.5
10	n_{wf}	4	1.2
11	k_{maxgf}	0.5	1.0
12	k_{maxwf}	0.1	0.75
13	ϕ	0.15	
14	S_{wrf}	0.15	
15	S_{wrm}	0.15	
16	S_{grf}	0.1	
17	S_{grm}	0.1	

1024
1025
1026

1027 Table 5 RMSE and relative RMSE of interactive linear surface models (ILRSM) at three
 1028 production stages for various MFHW Nf7 L600m Base Reference sets with different run
 1029 numbers and sampling approaches, i.e., Latin Hypercube, LHS, and two-level Full Factorial
 1030 Sampling, FFS.

	Run Numbers	LHS RMSE IL, 10 Days	Relative error % compare to LHS 4096 runs, 10 days	LHS RMSE IL, 30 Days	Relative error % compare to LHS 4096 runs, 30 days	LHS RMSE IL, 365 Days	Relative error % compare to LHS 4096 runs, 365 days
LHS 4096 Runs	4096	6.88	0.00	7.17	0.00	4.72	0.00
LHS 3000 Runs	3000	7.02	1.93	7.30	1.83	4.74	0.39
LHS 2000 Runs	2000	7.14	3.72	7.45	3.99	4.77	1.02
LHS 1000 Runs	1000	7.40	7.51	7.53	5.13	4.72	-0.04
LHS 500 Runs	500	7.87	14.27	7.78	8.64	4.69	-0.68
LHS 250 Runs	250	8.62	25.30	8.59	19.87	4.91	4.07
LHS 100 Runs	100	15.79	129.43	15.17	111.68	7.39	56.64
	Run Numbers	FF RMSE IL, 10 Days	Relative error % compare to LHS 4096 runs, 10 days	FF RMSE IL, 30 Days	Relative error % compare to LHS 4096 runs, 30 days	FF RMSE IL, 365 Days	Relative error % compare to LHS 4096 runs, 365 days
Full Factorial (4096 Runs)	4096	13.56	97.02	15.15	111.41	9.15	93.80

1031

1032 Table 6 RMSE and relative RMSE of the pure quadratic (PQ) model in run numbers for
 1033 MFHW Nf7 L600m Base Reference sets with LHS approach.

	Run Numbers	LHS RMSE PQ, 10 Days	Relative error % compare to LHS 4096 runs, 10 days	LHS RMSE PQ, 30 Days	Relative error % compare to LHS 4096 runs, 30 days	LHS RMSE PQ, 365 Days	Relative error % compare to LHS 4096 runs, 365 days
LHS 4096 Runs	4096	5.63	0.00	5.38	0.00	4.28	0.00
LHS 3000 Runs	3000	5.68	0.93	5.47	1.73	4.28	-0.07
LHS 2000 Runs	2000	5.68	0.93	5.46	1.48	4.27	-0.14
LHS 1000 Runs	1000	5.76	2.29	5.44	1.23	4.25	-0.76
LHS 500 Runs	500	5.75	2.09	5.45	1.35	4.28	0.00
LHS 250 Runs	250	5.94	5.47	5.58	3.71	4.30	0.57
LHS 100 Runs	100	6.03	7.02	5.95	10.69	4.33	1.08

1034

1035

1036 Table 7 RMSE and relative RMSE of the full quadratic (FQ) model in run numbers for
 1037 MFHW Nf7 L600m Base Reference sets with LHS approach.

	Run Numbers	LHS RMSE FQ, 10 Days	Relative error % compare to LHS 4096 runs, 10 days	LHS RMSE FQ, 30 Days	Relative error % compare to LHS 4096 runs, 30 days	LHS RMSE FQ, 365 Days	Relative error % compare to LHS 4096 runs, 365 days
LHS 4096 Runs	4096	4.13	0.00	4.49	0.00	4.26	0.00
LHS 3000 Runs	3000	4.22	2.27	4.59	2.22	4.26	0.02
LHS 2000 Runs	2000	4.35	5.44	4.67	3.92	4.27	0.20
LHS 1000 Runs	1000	4.41	6.80	4.74	5.45	4.20	-1.42
LHS 500 Runs	500	4.58	10.95	4.85	7.84	4.24	-0.42
LHS 250 Runs	250	5.74	38.94	5.52	22.84	4.39	3.04
LHS 100 Runs	100	13.32	222.62	10.88	142.17	4.33	1.62

1038

1039

1040 6. Figures

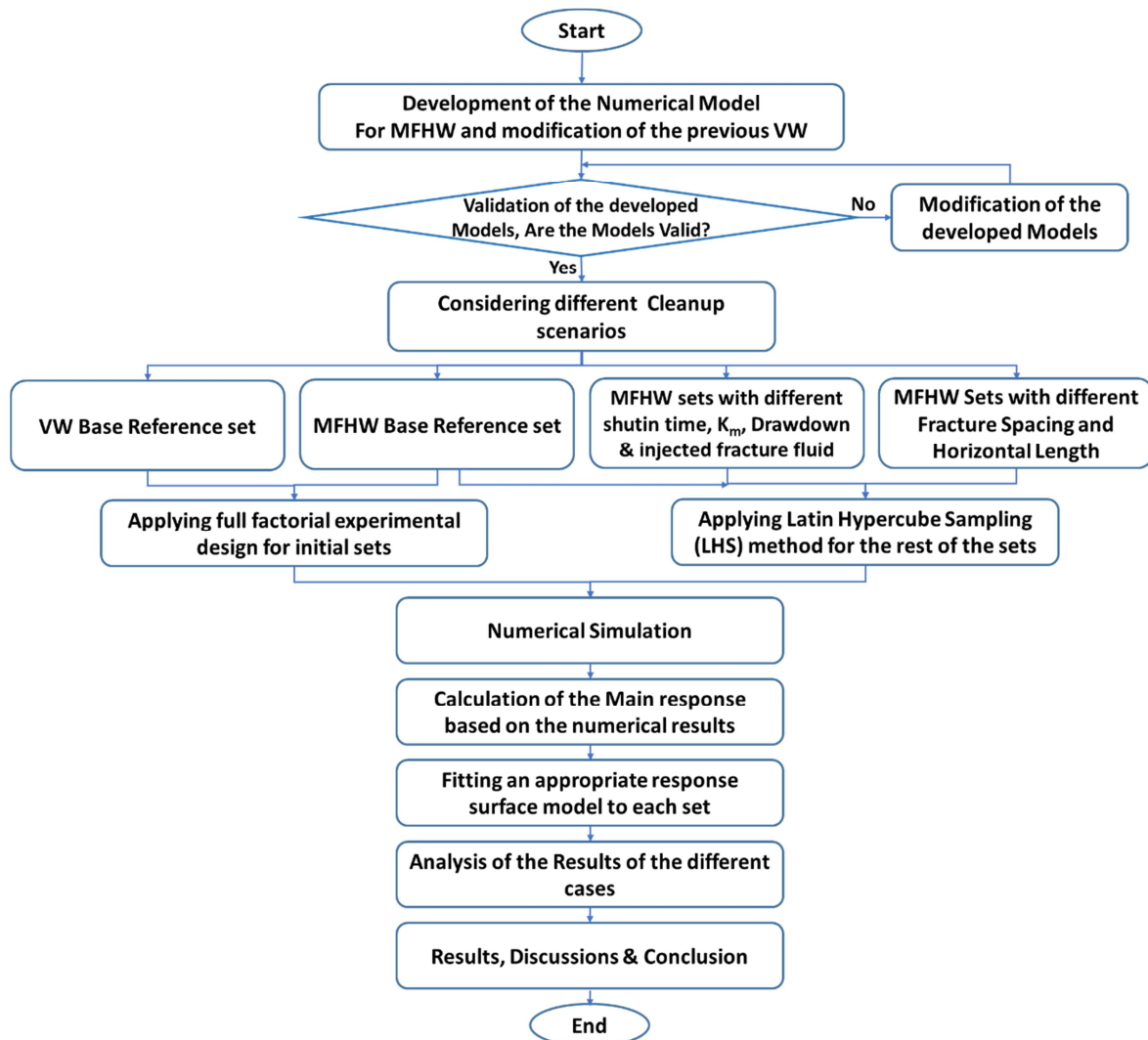


Figure 1 the workflow of the study

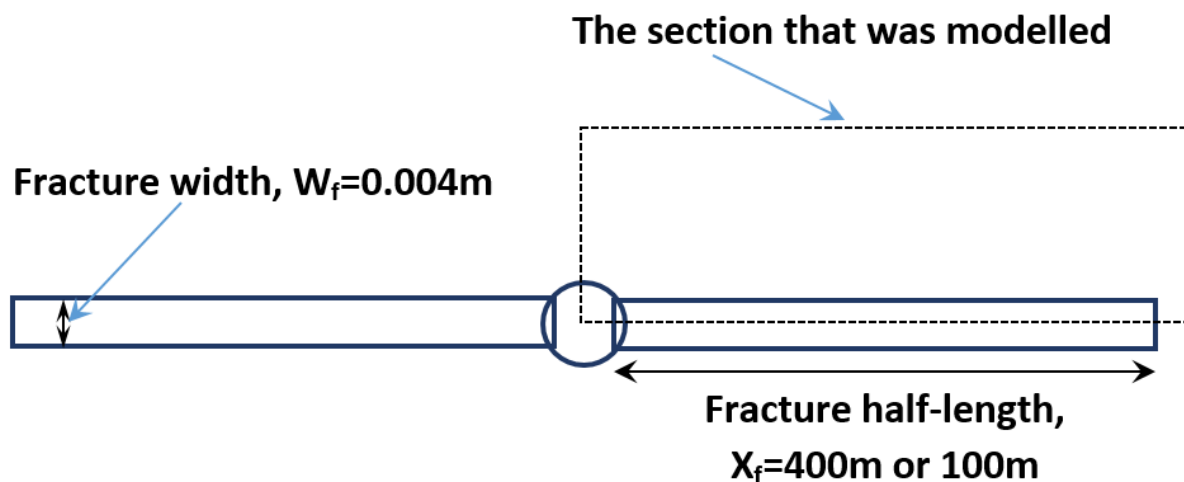


Figure 2 The modelled section

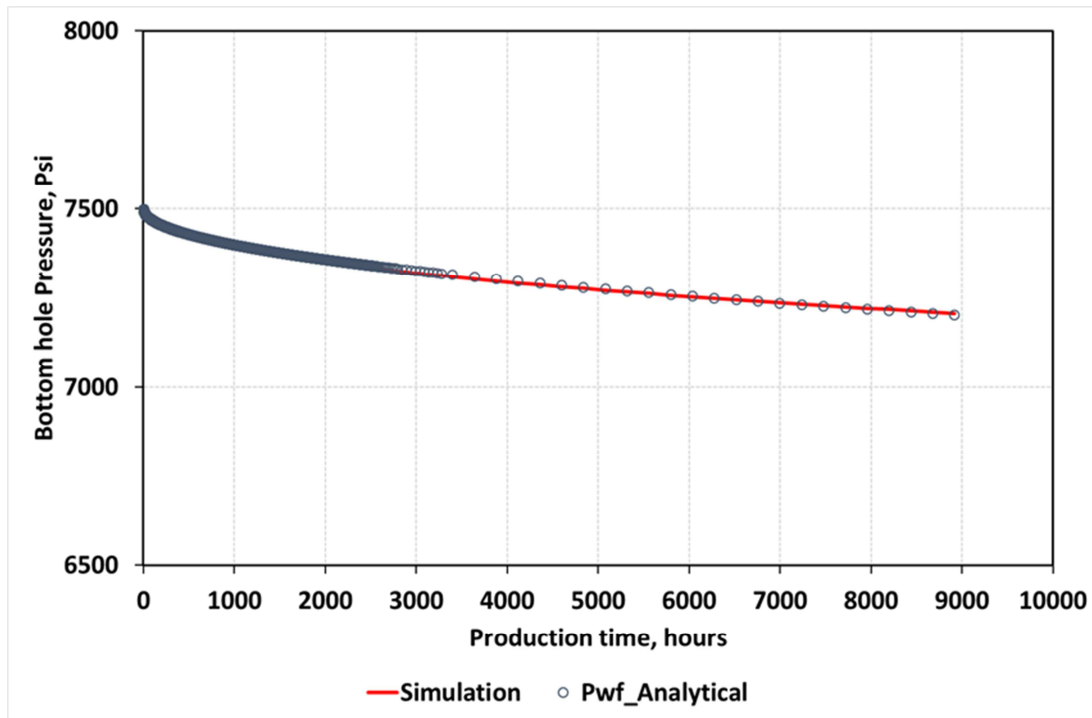


Figure 3 Predicated Pwf by numerical and analytical models versus time.

1041
1042
1043

VW and MFHW Base Reference Set, GPL - LRSM

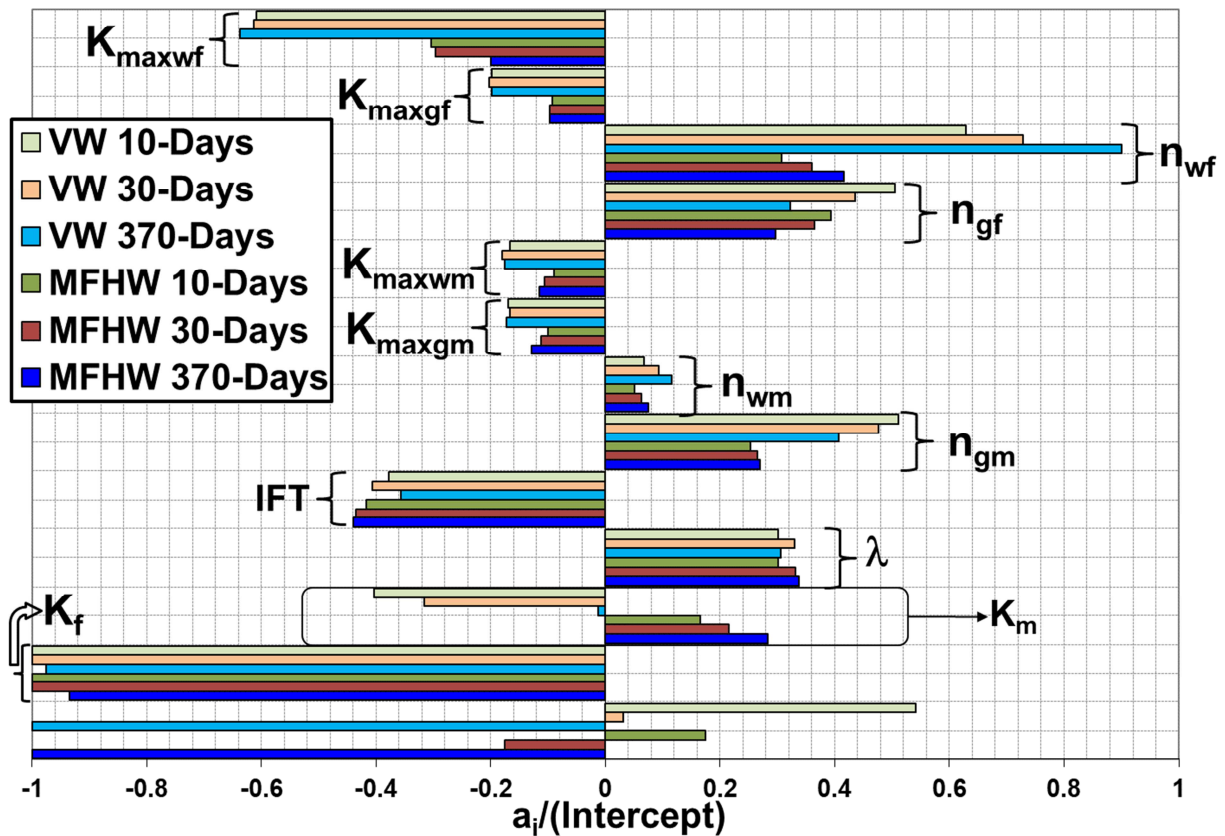


Figure 4 LRS coefficients, VW and MFHW Base Reference Sets (FVR=2, DP=1000 psi, ST=2 days and KMR=1).

1044
1045
1046

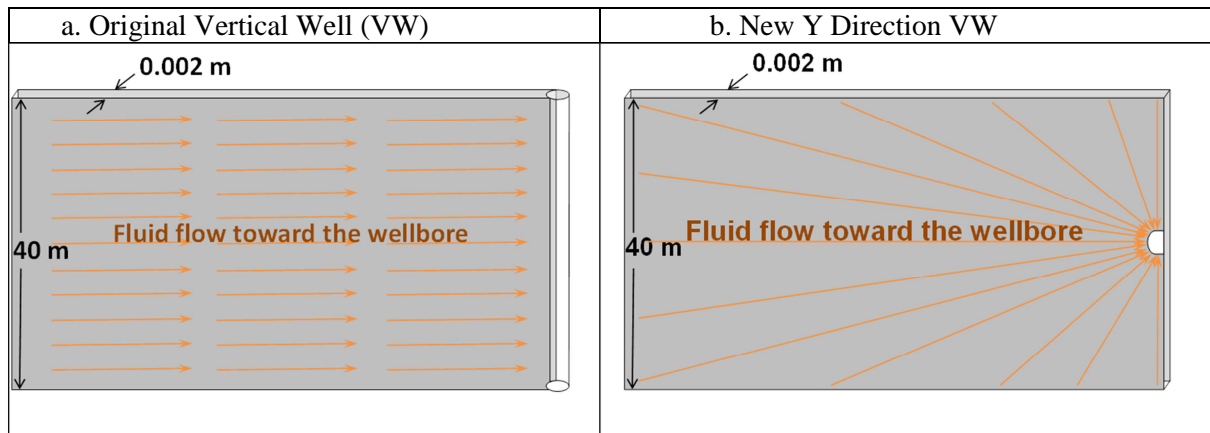


Figure 5 Well trajectory and flow geometry of Single Fracture (a) original Vertical Well (Z-VW) completed in the Z-direction, and (b) New VW completed in the Y- Direction (Y-VW).

1047

SFWW Base Reference Set, Y-Direction, Long Fracture, GPL- LRSM

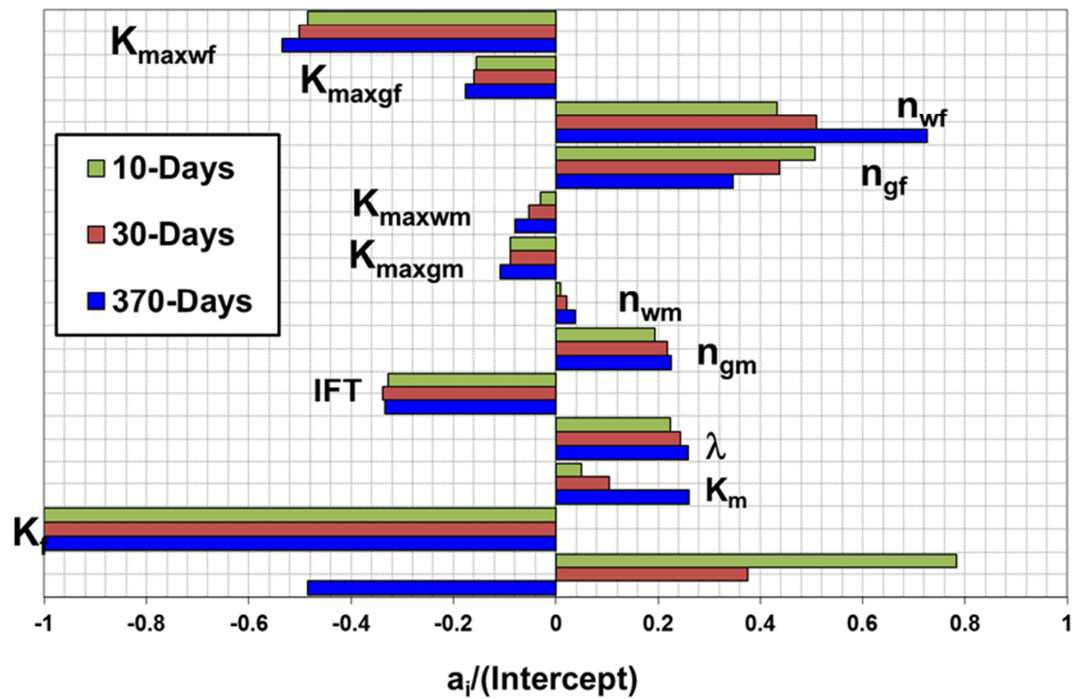


Figure 6 LRSM coefficients, at three production stages for the New Y-VW set.

1048

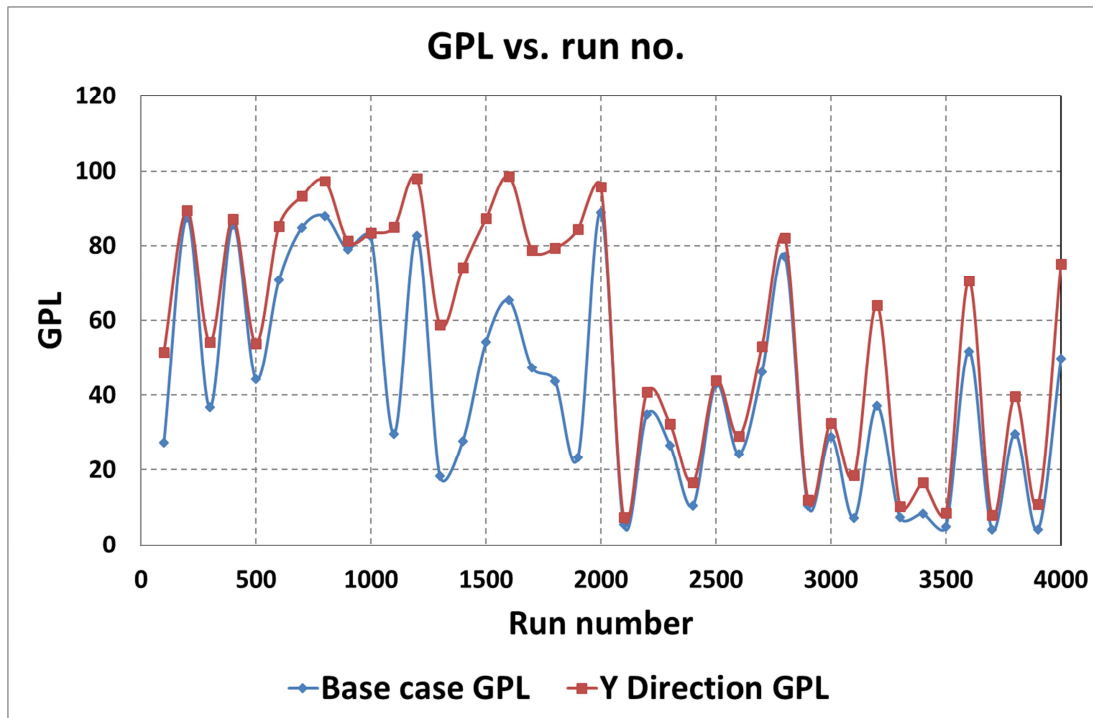


Figure 7 GPL vs Run Number for Z-VW and Y-VW sets,

1049

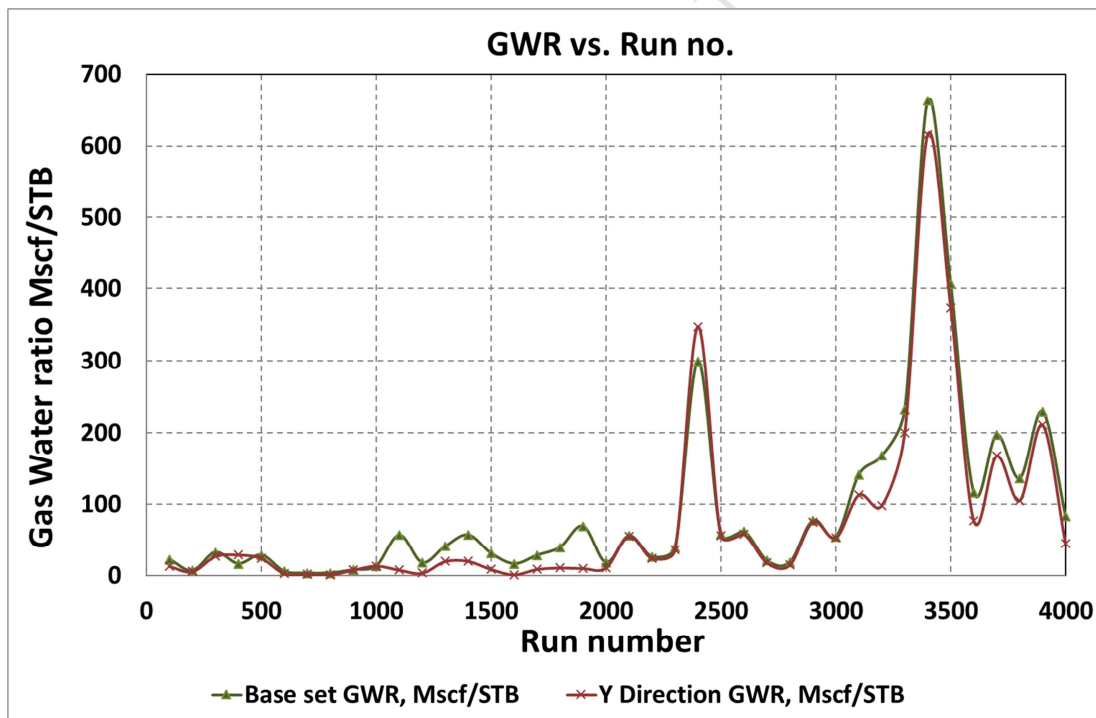


Figure 8 Gas Water Ratio vs Run Number for Z-VW and Y-VW sets,

1050

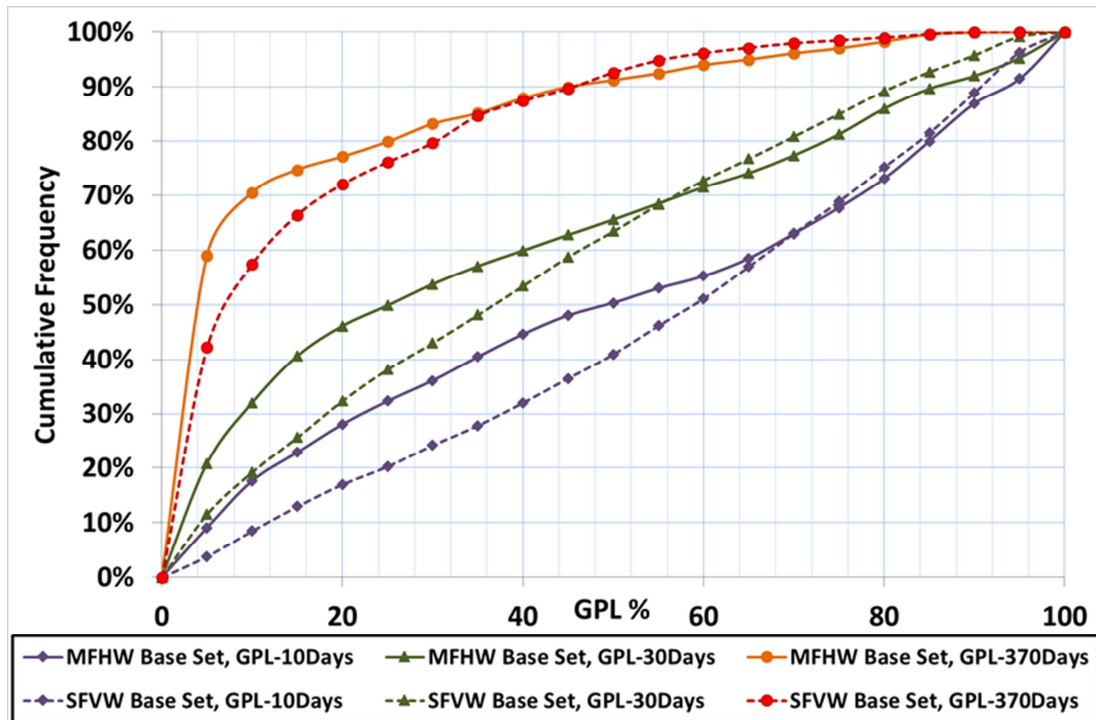


Figure 9 The GPL cumulative frequency of the MFHW set and VW Set at three production stages.

1051

MFHW-Set8 NF7-L600, Full Factorial Sampling, GPL-LRSM

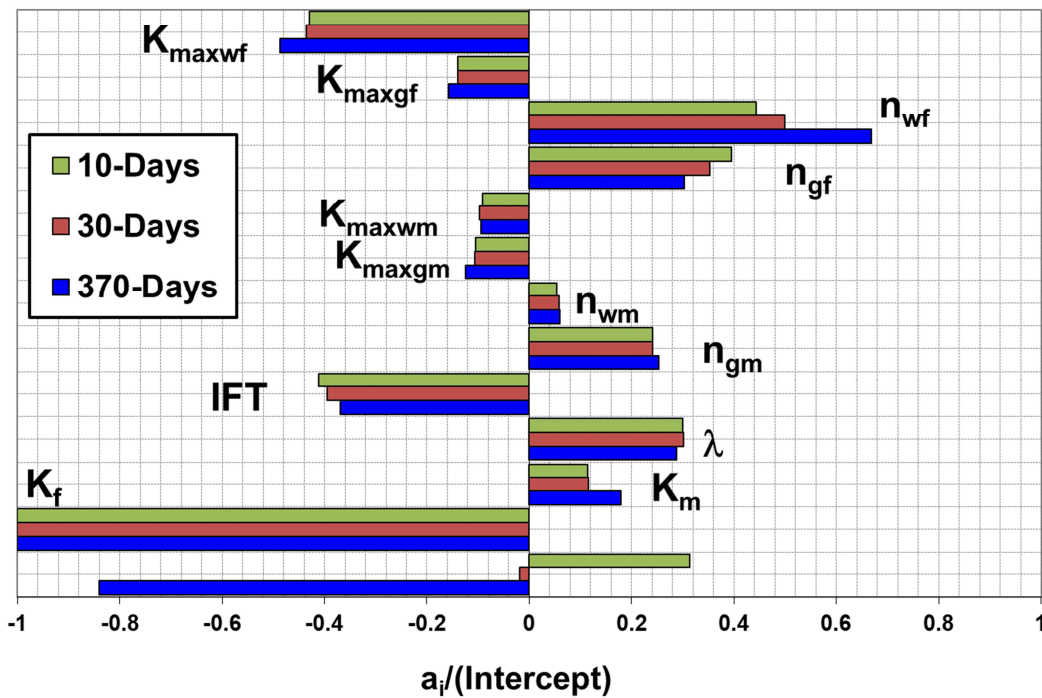


Figure 10 LRS coefficients , MFHW-Set8 Nf7 L600, Using FFS ,Base Reference Set,

1052

MFHW-Set23 NF7-L600, 4096 runs, Latin Hypercube , GPL- LRSM

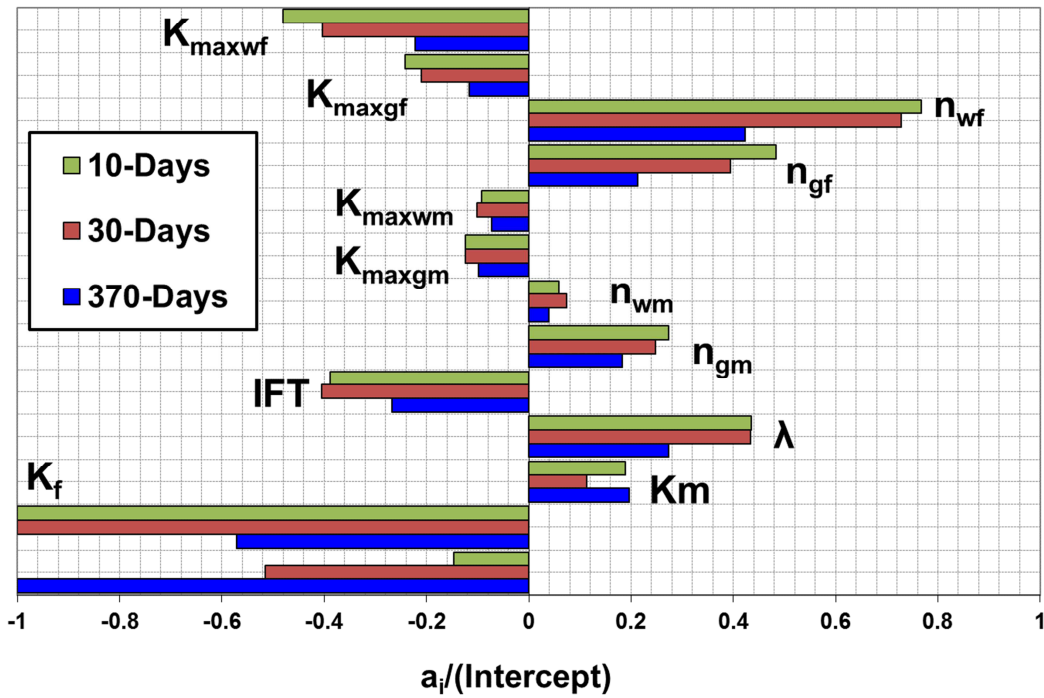


Figure 11 LRSM coefficients , MFHW-Set23 NF7 L600m Base Reference sets with LHS with 4096 Runs

1053
1054

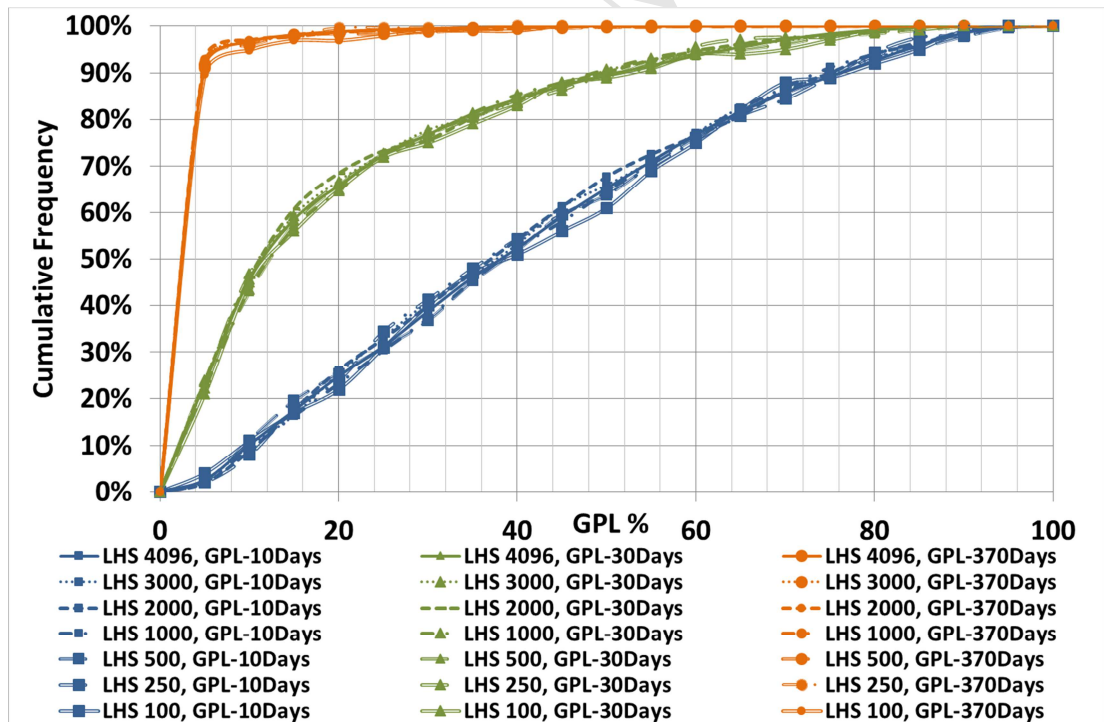


Figure 12 The GPL cumulative frequency of MFHW Base reference sets using LHS with different run numbers, (a) LHS with 4096 Runs, (b) LHS with 3000 Runs, (c) LHS with 2000 Runs, (d) LHS with 1000 Runs, (e) LHS with 500 Runs, (f) LHS with 250 Runs, (g) LHS with 100 Runs,

1055

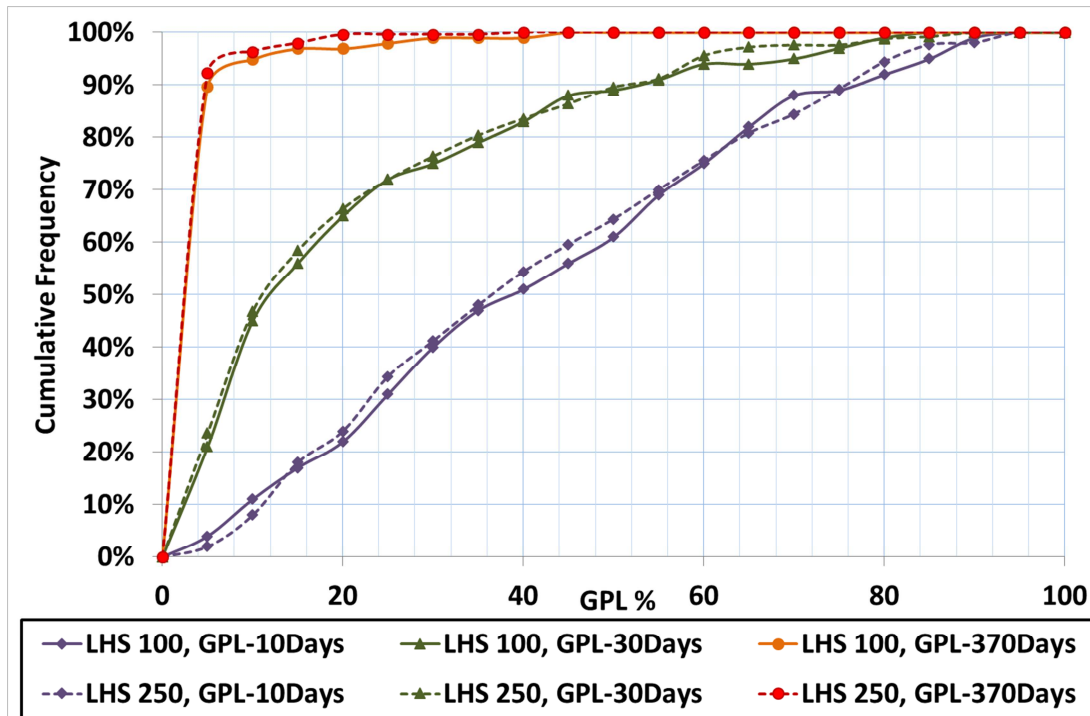


Figure 13 The GPL cumulative frequency of MFHW Base reference sets using LHS with 250 and 100 run numbers.

1056

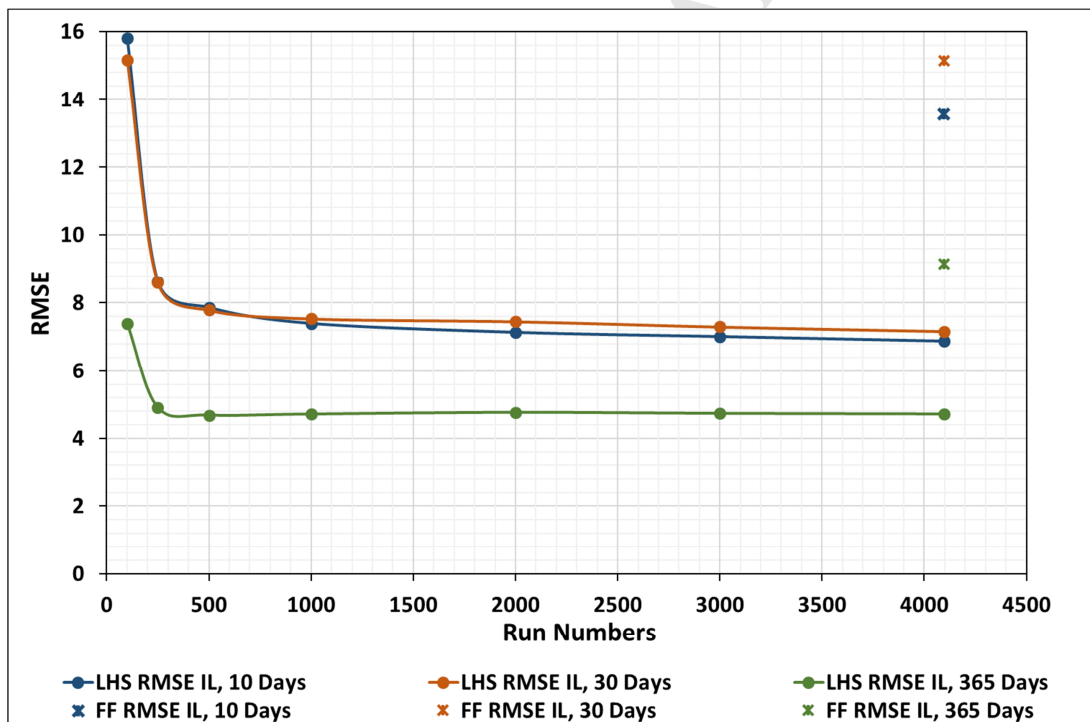


Figure 14 RMSE of interactive linear surface models (ILRSM) versus run numbers at three production stages for MFHW Nf7 L600m Base Reference sets with different sampling approaches, i.e., Latin Hyper Cube Sampling, LHS, and two level Full Factorial sampling (FFS)

1057

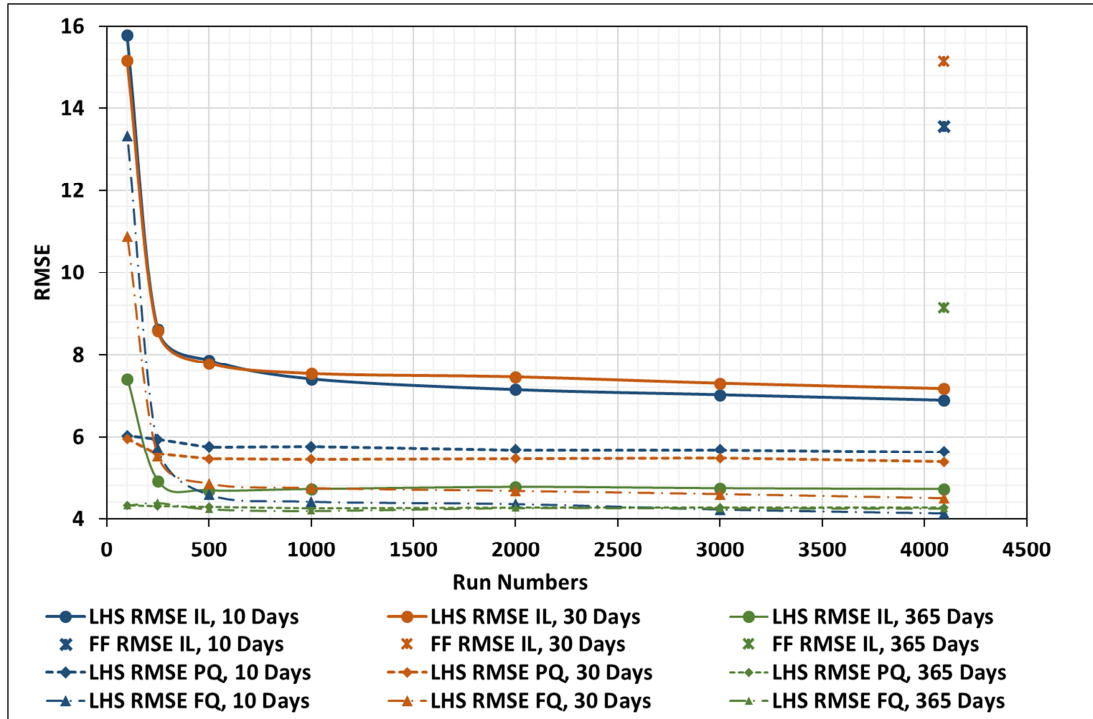


Figure 15 RMSE of ILRSM, pure quadratic (PQ) and full quadratic (FQ) models versus run numbers at three production stages for MFHW Nf7 L600m Base Reference sets with different sampling approaches, i.e., Latin HyperCube, LHS, and two level Full Factorial sampling (FFS)

1058

MFHW-Set 12 NF9 L600 Base Reference Set, GPL - LRSM

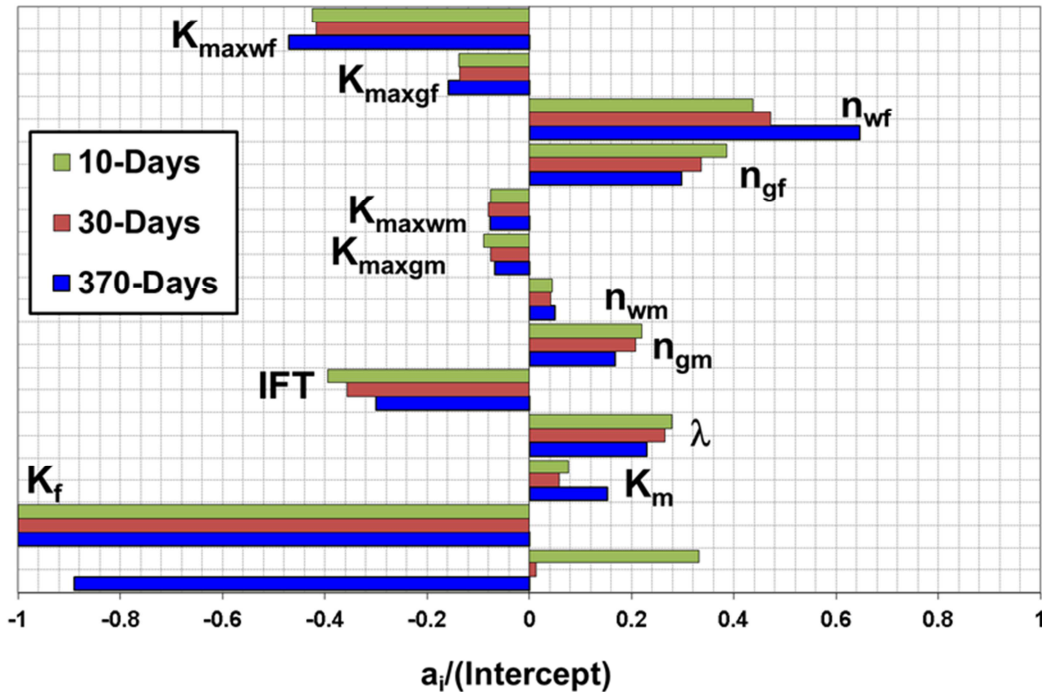


Figure 16 LRSM coefficients, MFHW-Set12 Nf9 L600

1059

MFHW-Set 13 NF13 L600 Base Reference Set, GPL - LRSM

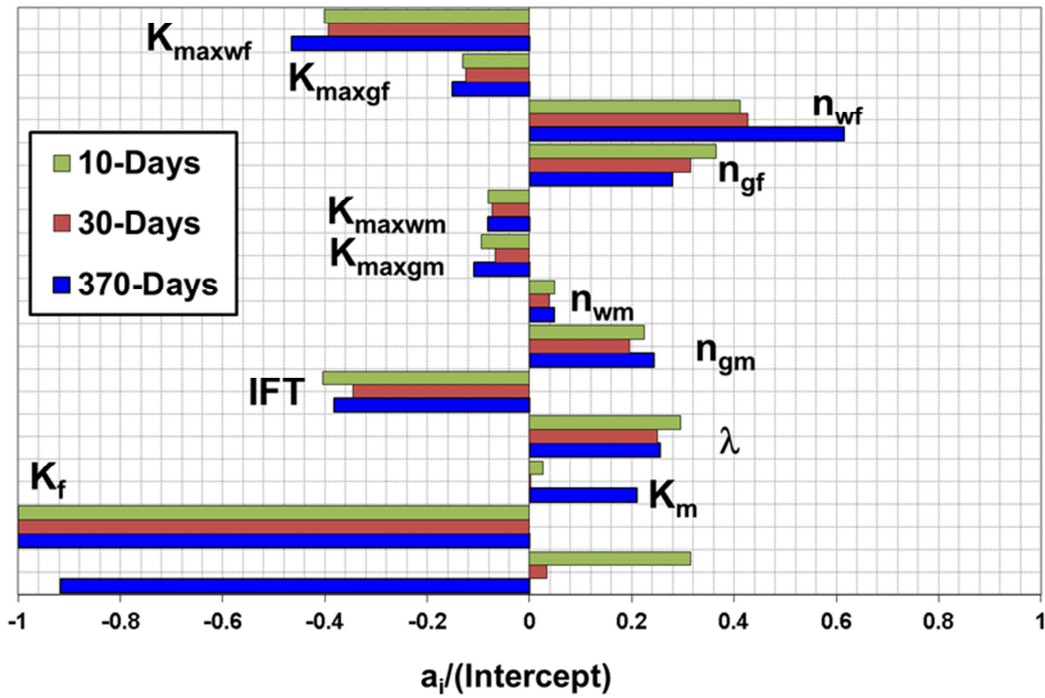


Figure 17 LRSM coefficients, MFHW-Set13 Nf13 L600

1060

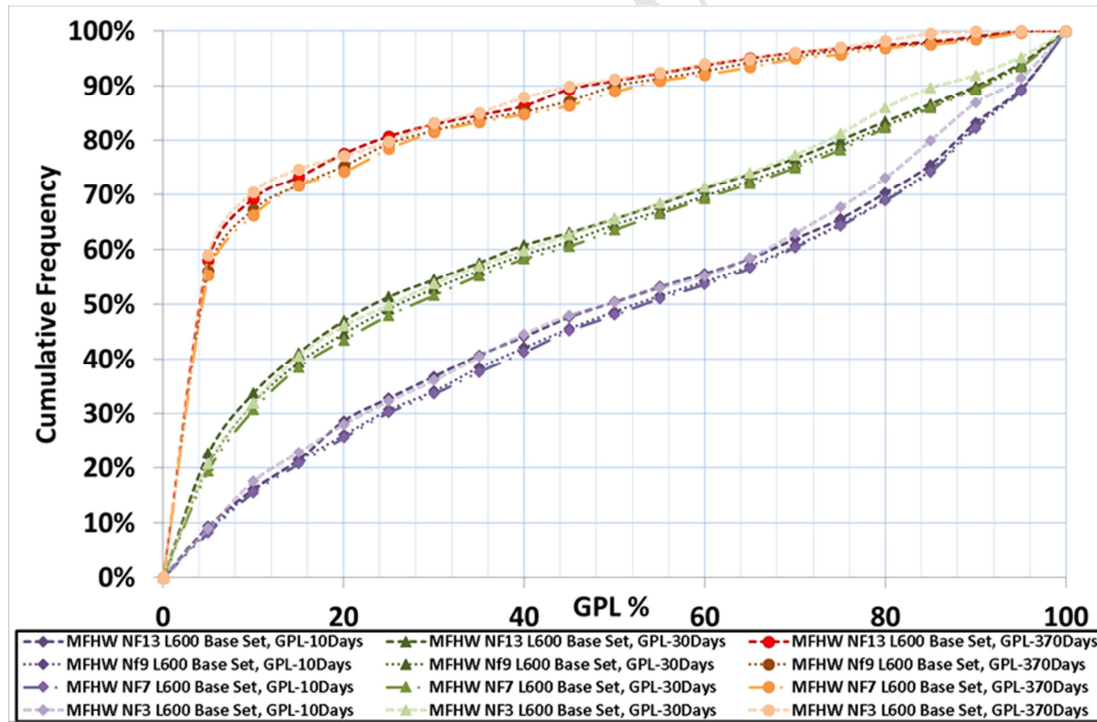


Figure 18 Histogram chart, GPL cumulative frequency of MFHW-Set 1Nf=3 & MFHW-Set 8 with Nf=7, MFHW-Set 12 with Nf=9 and MFHW-Set 13 with Nf=13 at three production stages.

1061

MFHW-Set14 NF10 L900 Base Reference Set, GPL - LRSM

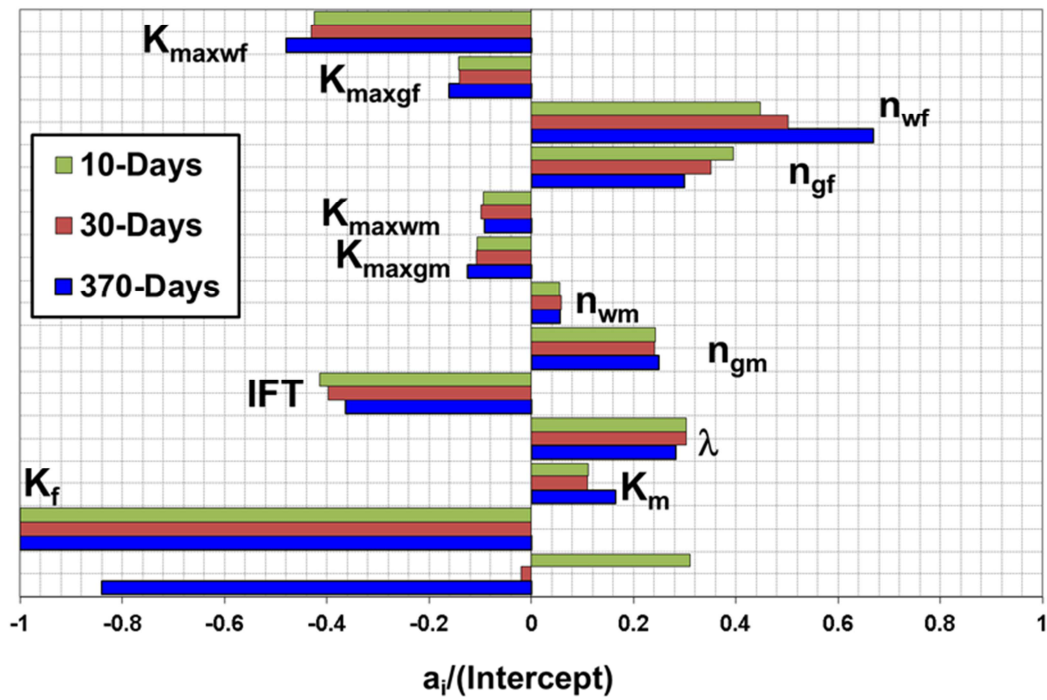


Figure 19 LRSM coefficients, MFHW-Set14 Nf10 L600

1062
1063
1064

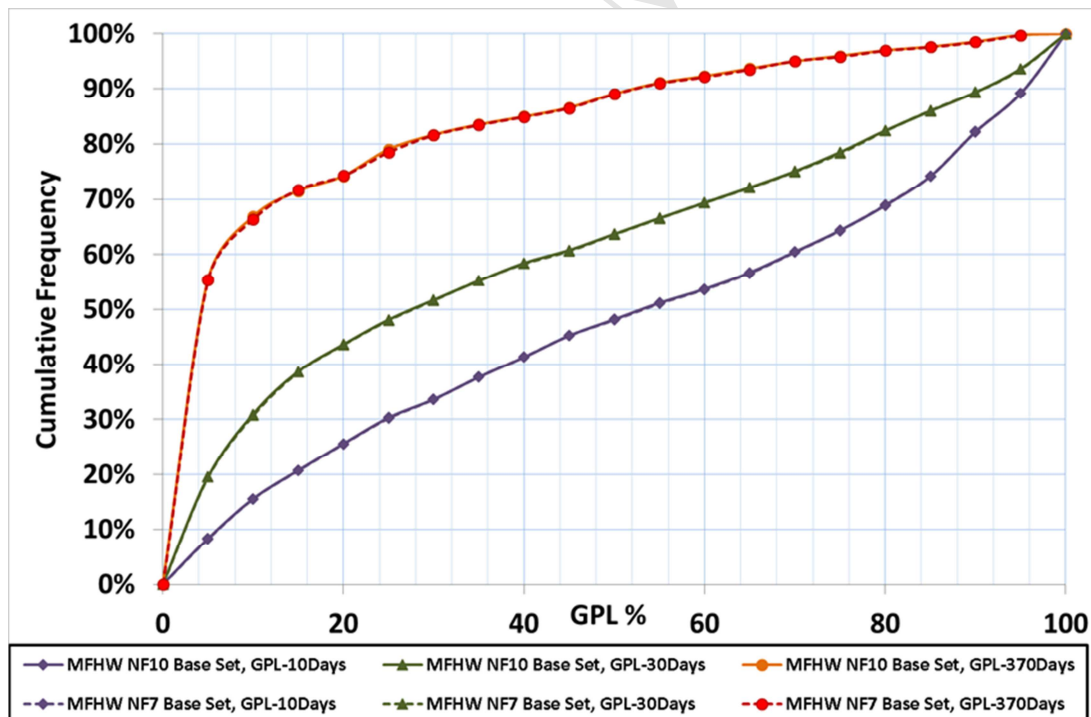
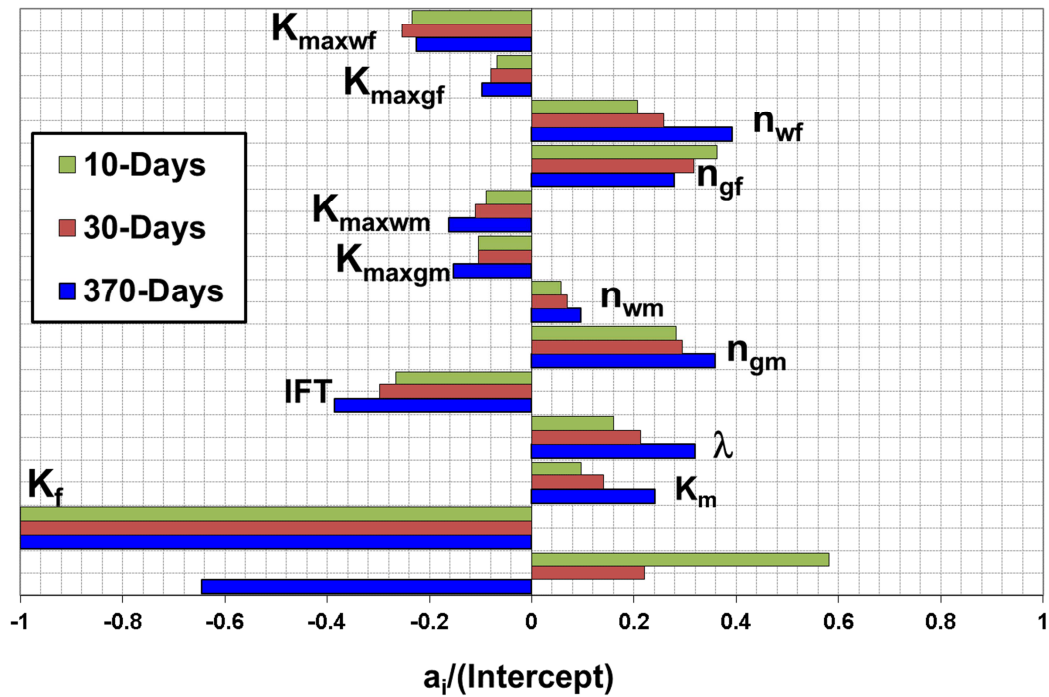


Figure 20 The GPL cumulative frequency of MFHW-Set 8 and Nf=7 & MFHW-Set 14 with Nf=10 at three production stages.

1065
1066
1067

a. MFHW-Set2 FVR=5

MFHW-Set 2, MFHW FVR=5, Gas Production Loss (GPL) - LRSM



b. SFVW-Set 9 FVR=5

SFVW-Set 9, FVR=5, Gas Production Loss (GPL) - LRSM

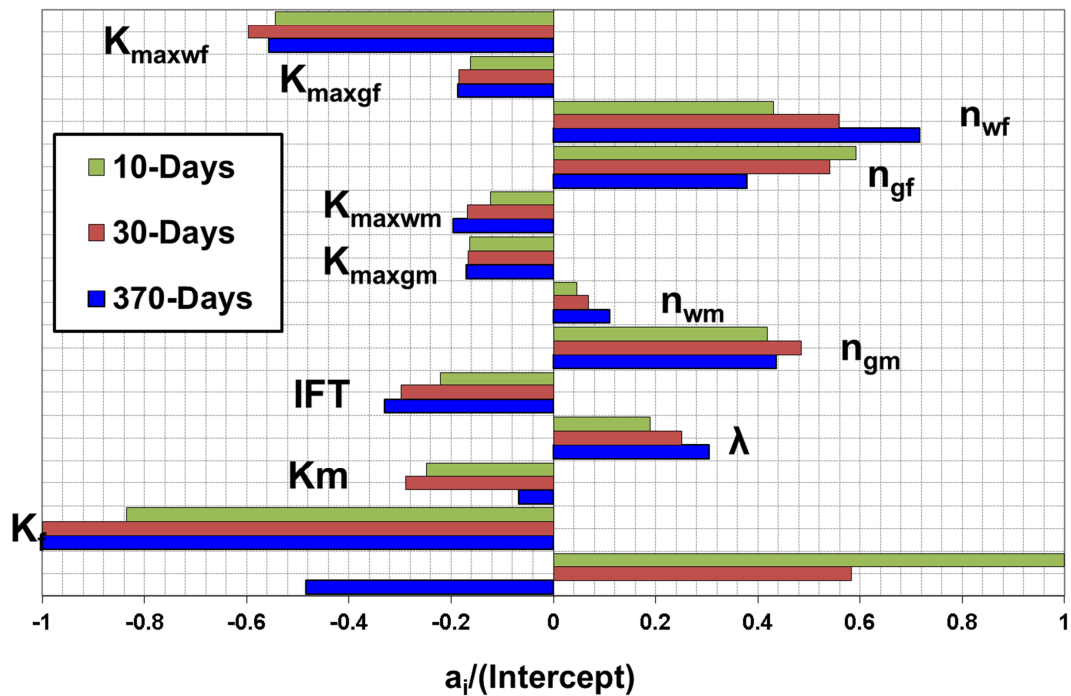


Figure 21 LRSM coefficients, (a)MFHW- Set 50 FVR=5 & (b) SFVW-Set9 FVR=5

1068
1069
1070

MFHW-Set 4, MFHW Kmr=10, Gas Production Loss (GPL) - LRSM

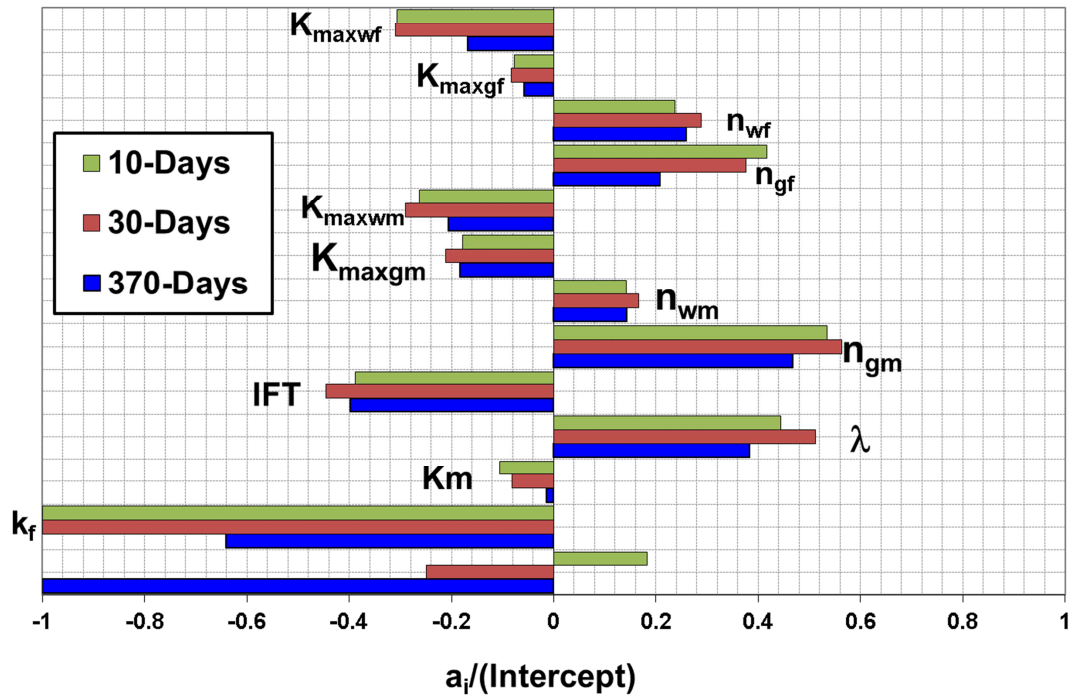
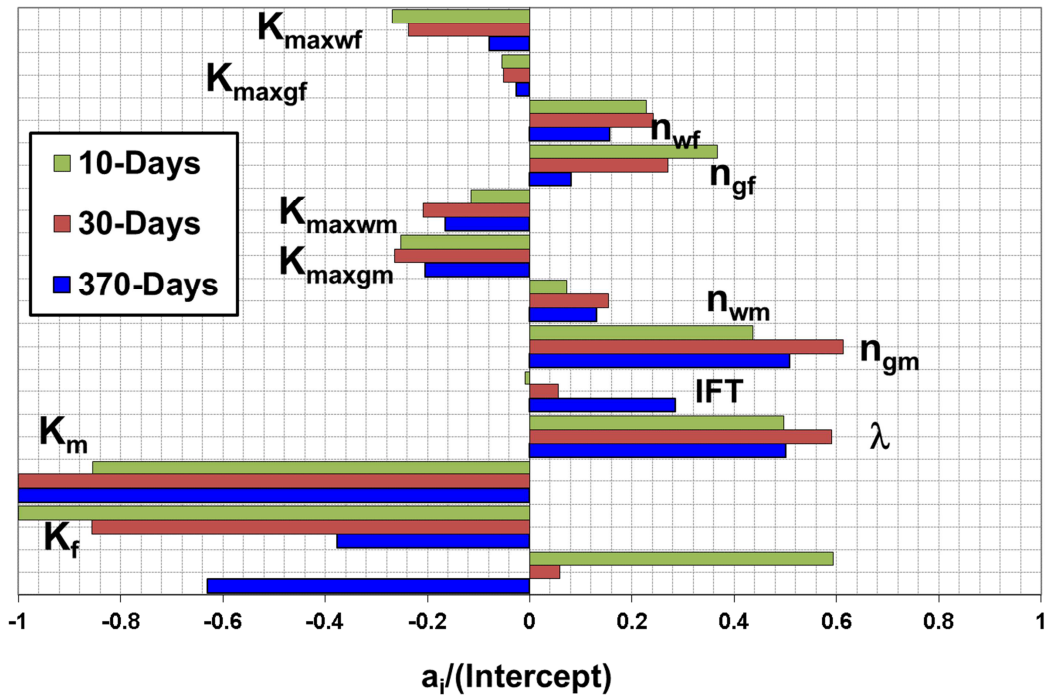


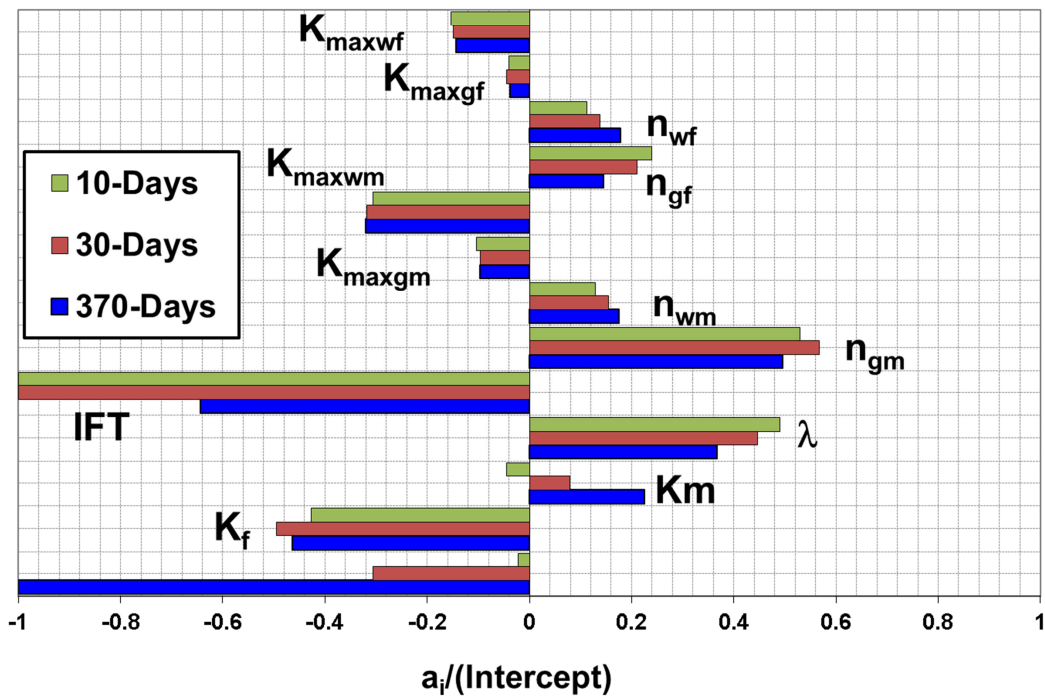
Figure 22 LRSM coefficients, MFHW KMR=10, MFHW-Set 4

1071

1072

MFHW-Set 7, MFHW $K_{mr}=100$, Gas Production Loss (GPL) - LRSMFigure 23 LRSM coefficients, MFHW $K_{MR}=100$, MFHW-Set 7

1073

MFHW-Set 5, MFHW $DP=100$, Gas Production Loss (GPL) - LRSMFigure 24 LRSM coefficients, MFHW $DP=100$, MFHW-Set 5

1074

1075

1076

MFHW-Set 6, MFHW DP=4000, Gas Production Loss (GPL) - LRSM

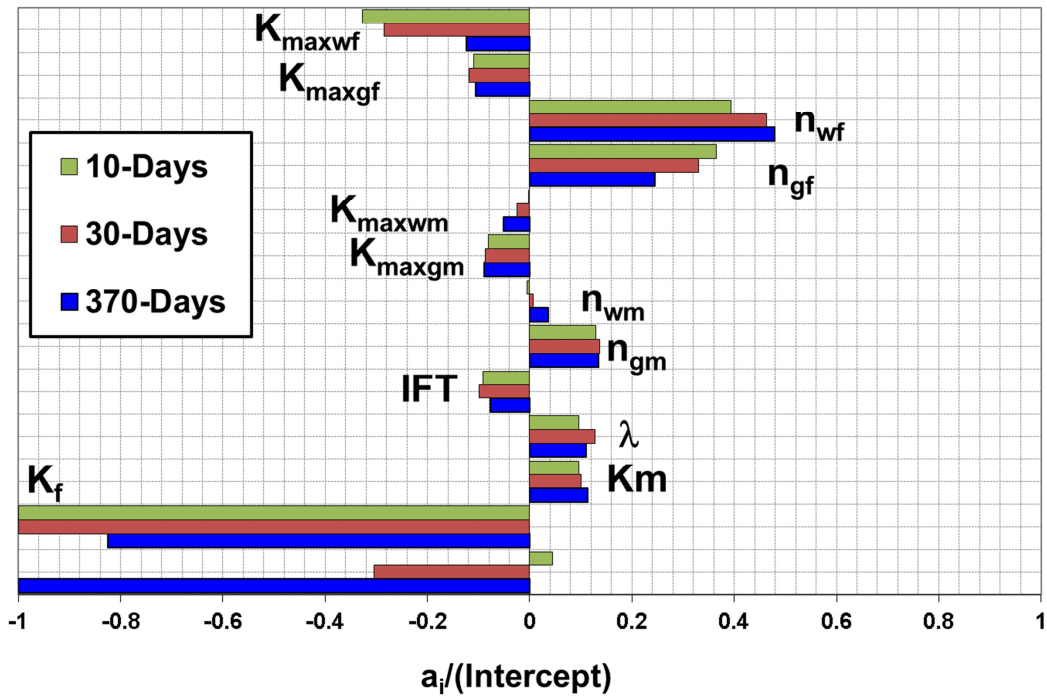


Figure 25 LRSM coefficients, MFHW DP=4000, MFHW-Set 6

1077

1078

1079

MFHW-Set9 Nf7 L600 Kmr=10, Gas Production Loss (GPL) - LRSM

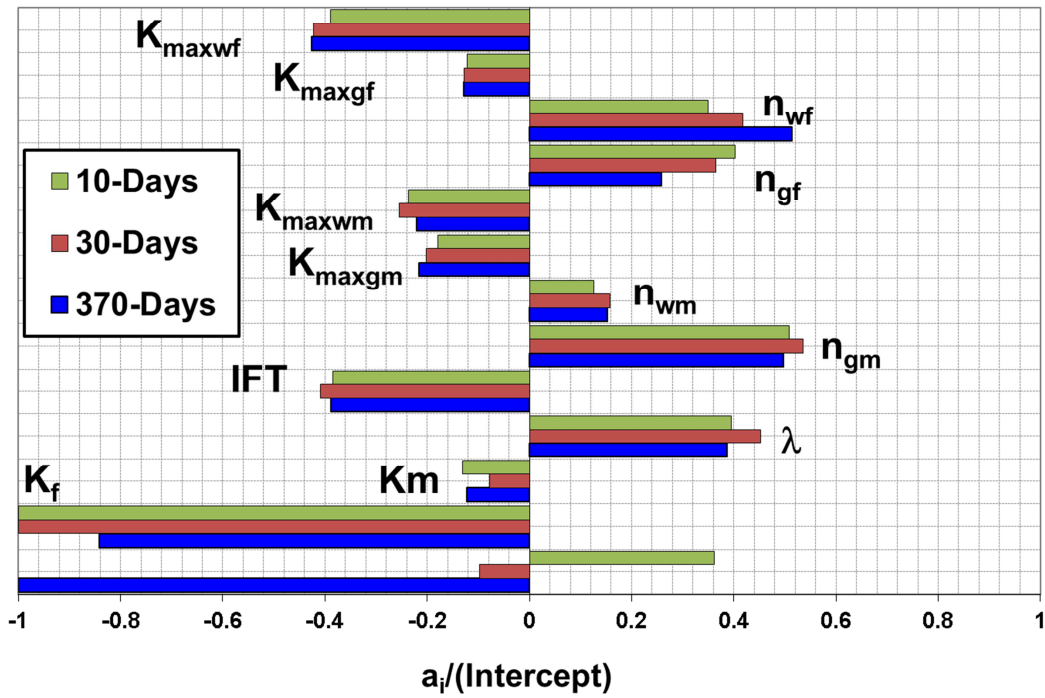


Figure 26 LRSM coefficients, MFHW-Set9 Nf7 L600 KMR=10, Base Reference Set

1080

MFHW-Set10 Nf7 L600 Kmr=100, Gas Production Loss (GPL) - LRSM

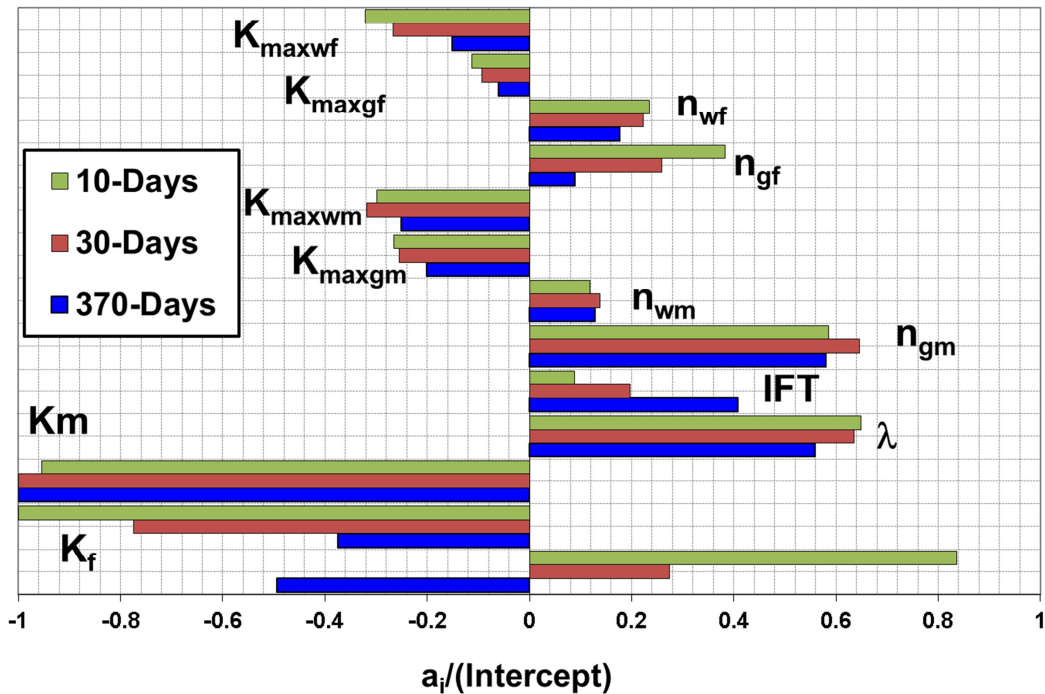


Figure 27 LRSM coefficients, MFHW-Set10 Nf7 L600 KMR=100, Base Reference Set

1081

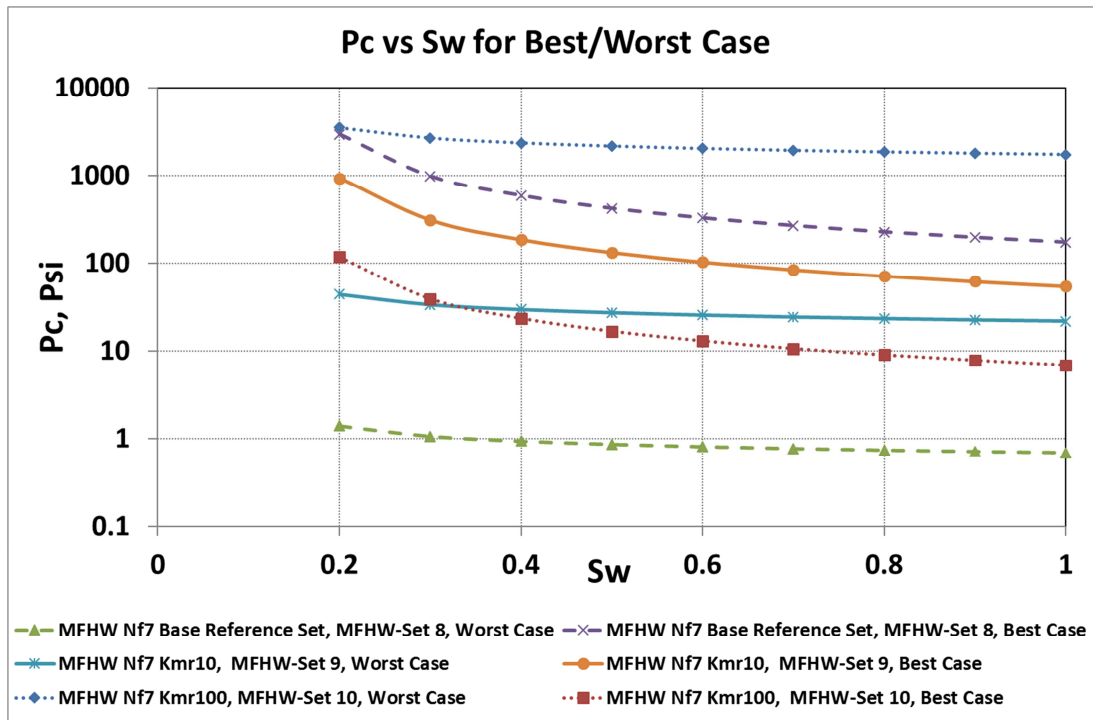


Figure 28 Pc vs. Sw for best/Worst Case of Sets MFHW-Set8, MFHW-Set9 and MFHW-Set10.

1082

MFHW-set15 Nf7-L600 DP4000, Gas Production Loss (GPL) - LRSM

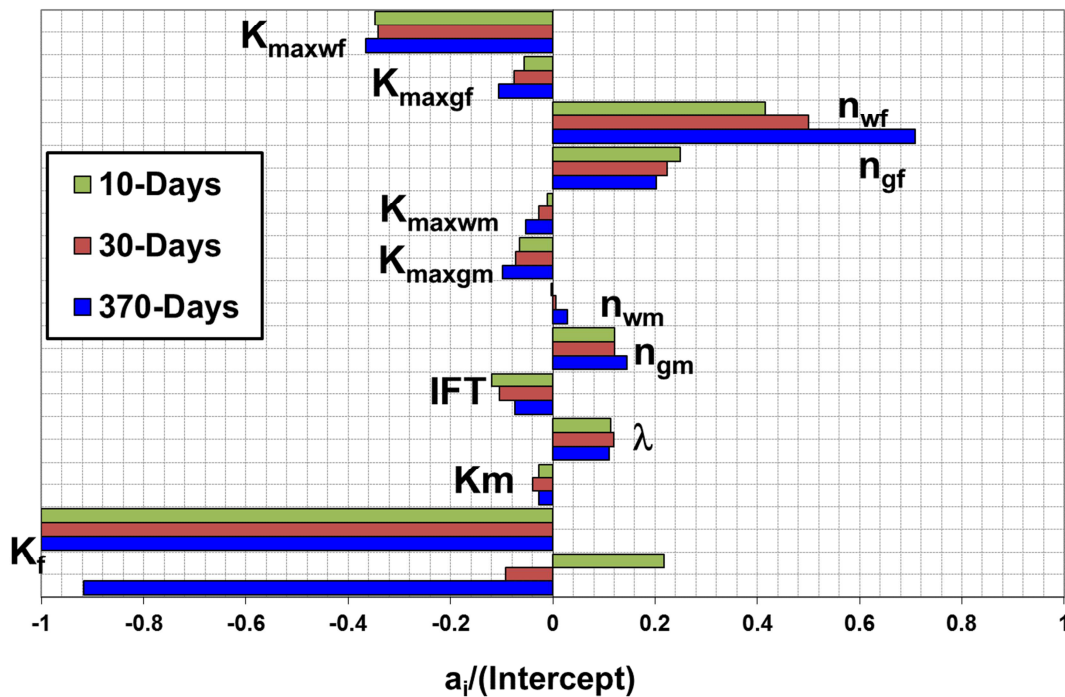


Figure 29 LRSM coefficients, MFHW-Set15 Nf7-L600m DP4000

1083

MFHW-set17 Nf7-L600 Kmr10DP4000, Gas Production Loss (GPL) - LRSM

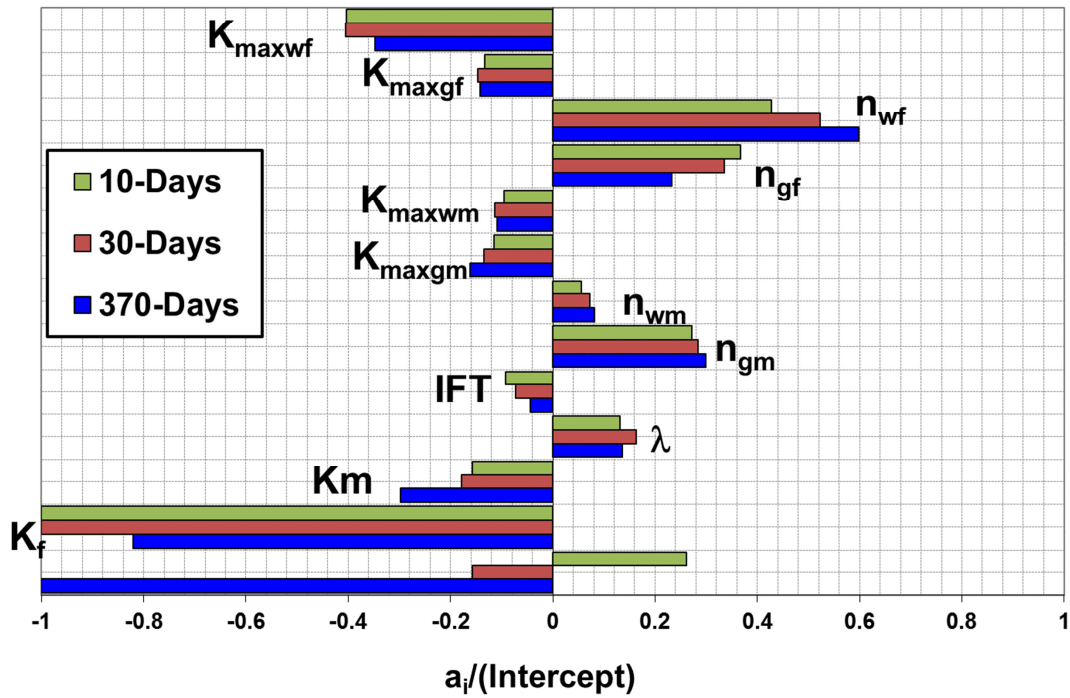


Figure 30 LRSM coefficients, MFHW-Set17 Nf7-L600m KMR10DP4000

1084

MFHW-set19 Nf7-L600 Kmr100DP4000, Gas Production Loss (GPL) - LRSM

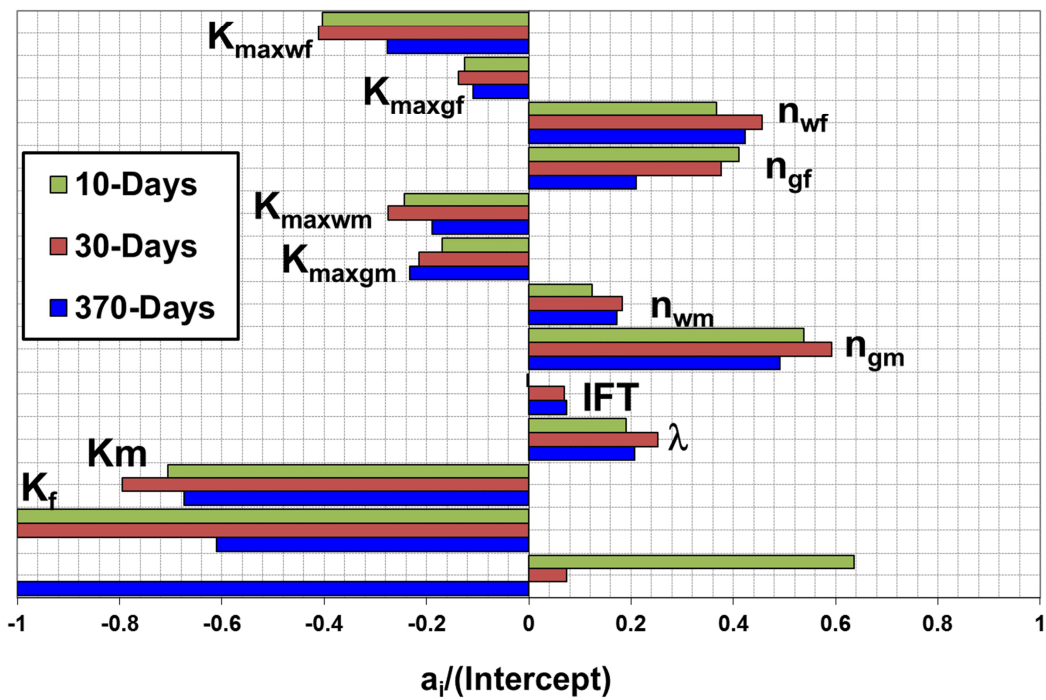


Figure 31 LRSM coefficients, MFHW-Set19 Nf7-L600m KMR100 DP4000

1085

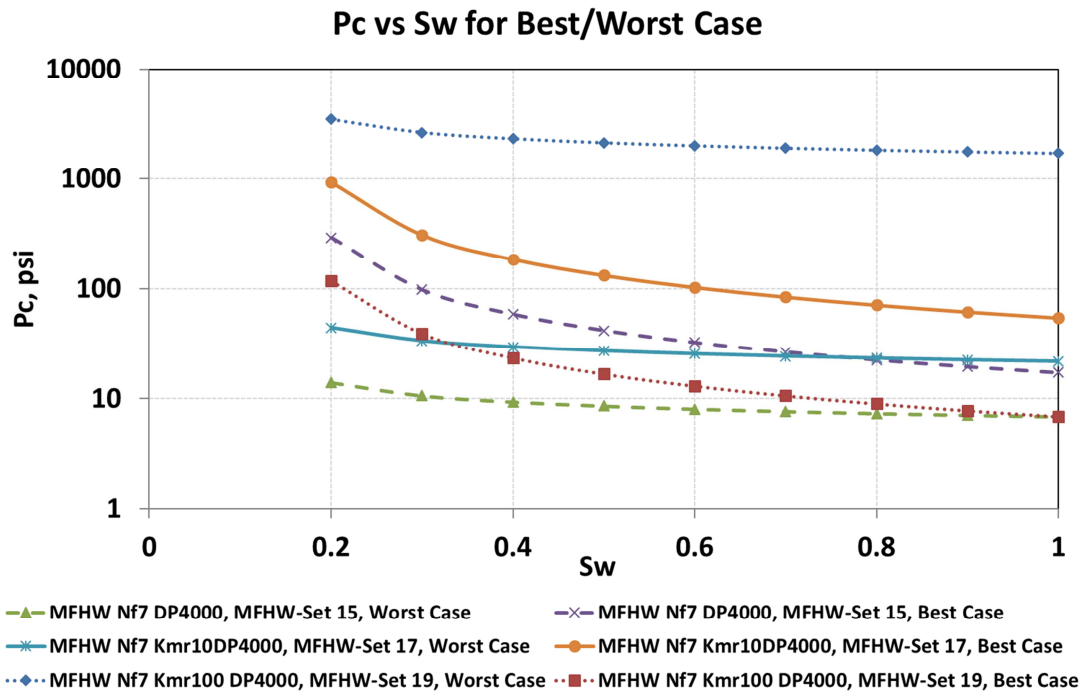


Figure 32 Pc vs. Sw for best/Worst Case of MFHW-Set15, MFHW-Set17 and MFHW-Set19

1086

MFHW-set11 Nf7 L600DP=100, Gas Production Loss (GPL) - LRSM

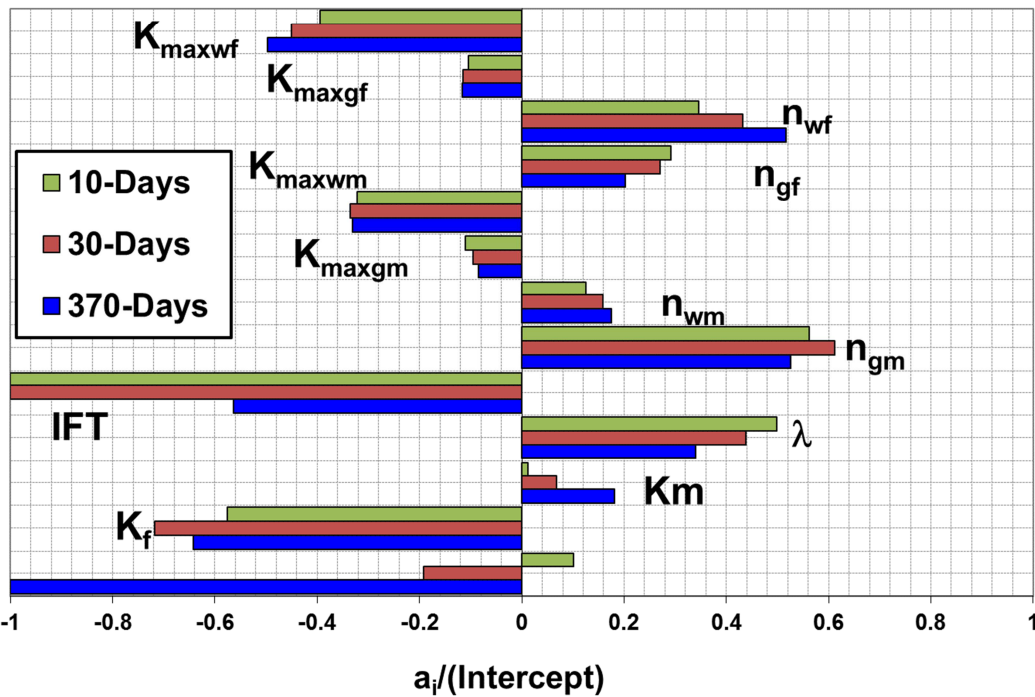


Figure 33 LRSM coefficients, MFHW-Set11 Nf7-L600m DP100

1087

MFHW-set16 Nf7 L600 Kmr=10DP100, Gas Production Loss (GPL) - LRSM

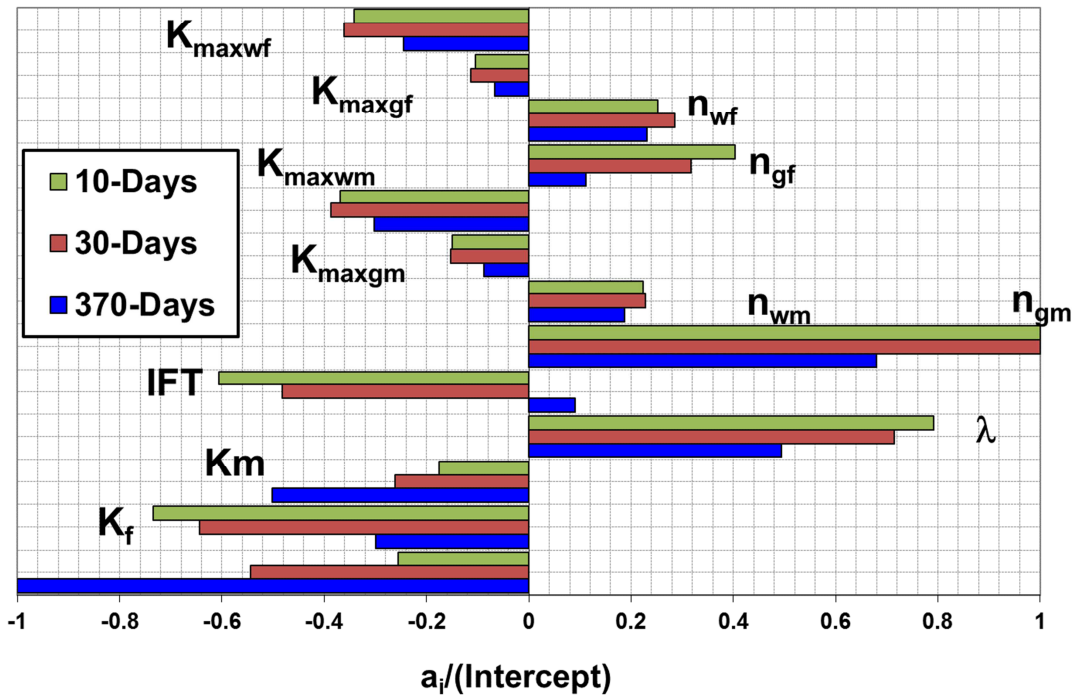


Figure 34 LRSM coefficients, MFHW-Set16 Nf7-L600m KMR10DP100

1088

MFHW-set18 Nf7-L600 Kmr=100DP100, Gas Production Loss (GPL) - LRSM

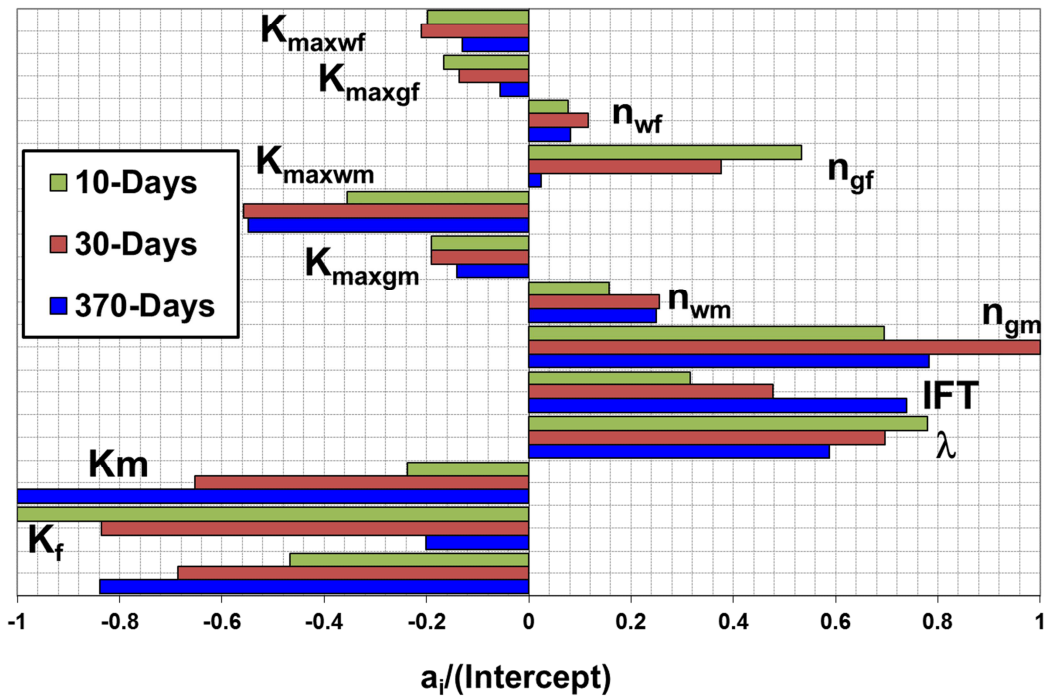


Figure 35 LRSM coefficients, MFHW-Set18 Nf7-L600m KMR100DP100

1089

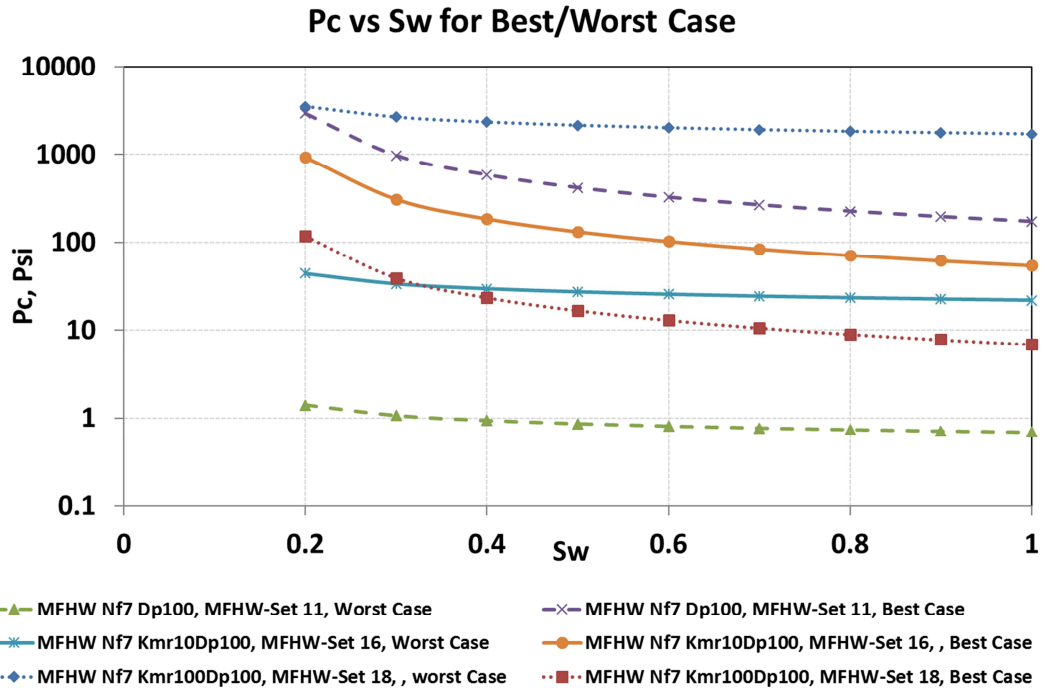


Figure 36 Pc vs. Sw for best/Worst Case of MFHW-Set11, MFHW-Set16 and MFHW-Set18

1090

1091

1092

1093

1094

1095

1096

Highlights

- An integrated investigation of clean-up efficiency of fractures was performed (in 30 new sets).
- Near wellbore choking effect in multiple fractured horizontal wells affects the cleanup mechanisms in a different way compared to vertical wells.
- Using IFT reducing agents is not recommended in tight formations whilst it is highly recommended to use such agents in ultratight formations.
- Although the impact of fracture interference/fracture spacing on flow is significant, its impact on clean-up performance is minimal.
- Latin Hypercube is a more realistic and reliable sampling approach compared to the two-level full-factorial experimental design.